Title: **Experimentally induced active and quiet sleep engage non-overlapping transcriptomes in *Drosophila***

Short title: **Active and quiet sleep in *Drosophila***

Authors: Niki Anthoney[1], Lucy A.L. Tainton-Heap[1], Hang Luong[2], Eleni Notaras[1], Qiongyi Zhao[1], Trent Perry[2], Philip Batterham[2], Paul J. Shaw[3] & Bruno van Swinderen[1*]

***Author Affiliation*:**

[1] Queensland Brain Institute, The University of Queensland, Brisbane, QLD 4072 Australia

[2] School of BioSciences, The University of Melbourne, Melbourne, VIC 3052 Australia

[3] Department of Neuroscience, Washington University School of Medicine, St. Louis, MO USA

Corresponding Author : b.vanswinderen@uq.edu.au

Abstract

Sleep in mammals is broadly classified into two different categories: rapid eye movement (REM) sleep and slow wave sleep (SWS), and accordingly REM and SWS are thought to achieve a different set of functions. The fruit fly *Drosophila melanogaster* is increasingly being used as a model to understand sleep functions, although it remains unclear if the fly brain also engages in different kinds of sleep as well. Here, we compare two commonly used approaches for studying sleep experimentally in *Drosophila*: optogenetic activation of sleep-promoting neurons and provision of a sleep-promoting drug, Gaboxadol. We find that these different sleep-induction methods have similar effects on increasing sleep duration, but divergent effects on brain activity. Transcriptomic analysis reveals that drug-induced deep sleep (‘quiet’ sleep) mostly downregulates metabolism genes, whereas optogenetic ‘active’ sleep upregulates a wide range of genes relevant to normal waking functions. This suggests that optogenetics and pharmacological induction of sleep in *Drosophila* promote different features of sleep, which engage different sets of genes to achieve their respective functions.

Introduction

There is increasing evidence that sleep is a complex phenomenon in most animals, comprising of distinct stages that are characterized by dramatically different physiological processes and brain activity signatures [1, 2]. This suggests that different sleep stages, such as rapid eye movement (REM) and slow-wave sleep (SWS) in humans and other mammals [3] are accomplishing distinct functions that are nevertheless collectively important for adaptive behavior and survival [4]. While REM and SWS appear to be restricted to a subset of vertebrates (e.g., mammals, birds, and possibly some reptiles [5-7] a broader range of animals, including invertebrates, demonstrate evidence of 'active' versus 'quiet' sleep, which could represent evolutionary antecedents of REM and SWS, respectively [1, 2, 8]. During active sleep, although animals are less responsive, brain recordings reveal a level of neural activity that is similar to wakefulness, in contrast to quiet sleep, which is characterized by significantly decreased neural activity in invertebrates [9, 10] as well as certain fish [11], mollusks [12], and reptiles [6].

Although it is likely that even insects such as fruit flies and honeybees sleep in distinct stages [13, 14], sleep studies using the genetic model *Drosophila melanogaster* still mostly measure sleep as a single phenomenon, defined by 5 minutes (or more) of inactivity [15, 16]. As sleep studies increasingly employ *Drosophila* to investigate molecular and cellular processes underpinning potential sleep functions, this simplified approach to measuring sleep in flies carries the risk of overlooking different functions accomplished by distinct kinds of sleep. Sleep physiology and functions are increasingly being addressed in the fly model by imposing experimentally controlled sleep regimes, either pharmacologically or via transient control of sleep-promoting circuits by using opto- or thermogenetic tools [17]. Yet, there is little knowledge available on whether these different approaches are producing qualitatively similar sleep. For example, sleep can be induced genetically in flies by activating sleep-

promoting neurons in the central complex (CX) – a part of the insect brain that has been found to be involved in multimodal sensory processing [18]. In particular, the dorsal fan-shaped body (dFB) of the CX has been found to serve as a discharge circuit for the insect's sleep homeostat, whereby increased sleep pressure (e.g., due to extended wakefulness) alters the physiological properties of dFB neurons causing them to fire more readily and thereby promote decreased behavioral responsiveness [19] and thus sleep [20-22]. Crucially, dFB activation was shown to be sleep-restorative [10, 23], but confusingly, brain recordings during dFB-induced sleep, via electrophysiology as well as whole-brain calcium imaging techniques, reveal wake-like levels of brain activity [9, 10]. This suggests that dFB-induced sleep might be promoting a form of sleep akin to the 'active' sleep stage detected during spontaneous sleep [9, 10].

An alternate way to induce sleep in *Drosophila* is by feeding flies the GABA-agonist 4,5,6,7-tetrahyrdoisoxazolopyridin-3-ol, (THIP), also known as Gaboxadol. Several studies have shown that THIP-induced sleep is also restorative and achieves key functions ranging from memory consolidation to cellular repair and waste clearance [23-26]. This pharmacological approach centered on GABA function has a solid foundation based on better-understood sleep processes: in mammals, many sleep-inducing drugs also target GABA receptors, and this class of drugs tends to promote SWS [27]. In contrast, there are no obvious drugs that promote REM sleep, although local infusion of cholinergic agonists (e.g., carbachol) to the brainstem has been shown to induce REM-like states in cats [28].

In this study, we compare THIP-induced sleep with dFB-induced sleep in *Drosophila*, using behavior, brain activity, and transcriptomics. To ensure the validity of our comparisons, we performed all of our experiments in the same genetic background, employing a canonical Gal4 strain that expresses a transgenic cation channel in the dFB: R23E10-Gal4 > UAS-Chrimson [29, 30]. When these flies are fed all-trans-retinal (ATR) and then exposed to red light, they are put to sleep optogenetically. When these flies are instead fed THIP, they are put

to sleep pharmacologically. By using the same genetic background, we were thus able to contrast the effects of either kind of sleep at the level of behavior, brain activity, and gene expression (**Figure 1**).

Materials and Methods

Animals

Drosophila melanogaster flies were reared in vials (groups of 20 flies / vial) on standard yeast-based medium under a 12:12 light/dark (8 AM:8 PM) cycle and maintained at 25°C with 50% humidity. Adult, 3-5 day-old female, flies were used for all experiments and randomly assigned to experimental groups. Fly lines used for behavioral and RNA-sequencing experiments include R23E10-Gal4 (attp2; Bloomington 49032; Bloomington Drosophila Stock Center, Bloomington, Indiana) and UAS-CsChrimson-mVenus (attp18; Bloomington 55134; Provided by Janelia Research Campus, Ashburn, Virginia)[30]. For all 2-photon experiments, flies with the genotype 10XUAS-Chrimson88-tdTomato (attp18) / +: LexAop-nlsGCaMP6f (VIE-260b; kindly provided by Barry J. Dickson) / +: Nsyb-LexA (attP2) [31], LexAop-PAGFP (VK00005) / R23E10-Gal4 were used. Optogenetically-manipulated fly lines were maintained on food containing 0.5mg/ml all-trans retinal (ATR; Merck, Darmstadt, Germany) for 24 hours prior to assay to allow for sufficient consumption. Pharmacologically-manipulated flies were maintained on food with 0.1 mg/ml of Gaboxadol (4,5,6,7-tetrahyrdoisoxazolopyridin-3-ol, THIP) for the duration of behavioral experiment [23].

2-photon imaging

2-photon imaging was performed as described previously [10] using a ThorLabs Bergamo series 2 multiphoton microscope. Fluorescence was detected with a High Sensitivity GaAsP

photomultiplier tube (ThorLabs, PMT2000). GCaMP fluorescence was filtered through the microscope with a 594 dichroic beam splitter and a 525/25nm band pass filter.

For imaging experiments, flies were secured to a custom-built holder (REF). Extracellular fluid (ECF) containing 103 NaCl, 10.5 trehalose, 10 glucose, 26 NaHCO3, 5 C6H15NO6S, 5 MgCl2 (hexa-hydrate), 2 Sucrose, 3 KCl, 1.5 CaCl (dihydrate), and 1 NaH2PO4 (in mM) at room temperature was used to fill a chamber over the head of the fly. The brain was accessed by removing the cuticle of the fly with forceps, and the perineural sheath was removed with a microlance. Flies were allowed to recover from this for one hour before commencement of experiments. Imaging was performed across 18 z-slices, separated by 6µm, with two additional flyback frames. The entire nlsGCaMP6f signal was located within a 256 x 256px area, corresponding to 667 x 667µm. Fly behavior was recorded with a Firefly MV 0.3MP camera (FMVU-03MTM-CS, FLIR Systems), which was mounted to a 75mm optical lens and an infrared filter. Camera illumination was provided by a custom-built infrared array consisting of 24 3mm infrared diodes. Behavioral data was collected for the duration of all experiments.

For THIP experiments, an initial five minutes of baseline activity was captured, followed by perfusion of 0.2mg/ml THIP in ECF onto the brain at a rate of 1.25ml/minute for five minutes. An additional twenty minutes of both brain and behavioral activity were recorded to allow visualization of the fly falling asleep on the ball as a result of THIP exposure.

Behavioral responsiveness probing

For probing behavioral responsiveness in the brain imaging preparation, flies walking on an air-supported ball were subjected to a 50ms long, 10psi air puff stimulus, which was generated using a custom-built apparatus and delivered through a 3mm-diameter tube onto the front of the fly. Flies were subjected to 10 pre-THIP stimuli at a rate of one puff/minute, to characterize the baseline response rate. Flies were then perfused with 0.2mg/ml THIP in

ECF for five minutes, followed by continuous ECF perfusion for the remaining experimental time. Five minutes after the fly had fallen asleep on the ball, a further 20 air puff stimuli were delivered, at a rate of one puff/minute. Behavioral responses to the air puff were noted as a 'yes' (1) or 'no' (0), which were characterized as the fly rapidly walking on the ball immediately following the air puff. For statistical analysis, the pre-THIP condition was compared to either the first or last 10 minutes of the post-THIP condition.

Imaging analysis

Preprocessing of images was carried out using custom written Matlab scripts and ImageJ. Motion artifacts of the images were corrected as described previously [10]. Image registration was achieved using efficient sub-pixel image registration by cross-correlation. Each z-slice in a volume (18 z-slices and 2 flyback slices) is acquired at a slightly different time point compared to the rest of the slices. Hence to perform volume (x,y,z) analysis of images, all the slices within a volume need to be adjusted for timing differences. This was achieved by using the 9^{th} z-slice as the reference slice and temporal interpolation was performed for all the other z-slices using 'sinc' interpolation. The timing correction approach implemented here is conceptually similar to the methods using in fMRI for slice timing correction.

For each individual z-slice, a standard deviation projection of the entire time series was used for watershed segmentation with the 'Morphological segmentation' ImageJ plugin [32]. Using a custom-written MatLab (Mathworks) code, the mean fluorescent value of all pixels within a given ROI were extracted for the entire time series, resulting in a n x t array for each slice of each experiment, where n refers to the number of neurons in each Z-slice, and t refers to the length of the experiment in time frames. These greyscale values were z-scored for each neuron, and the z-scored data was transformed into a binary matrix where a value of > 3 standard

157 deviations of the mean was allocated a '1', and every value < 3 standard deviations was
158 allocated a '0'. To determine whether a neuron fired during the entire time series, a rolling sum
159 of the binary matrix was performed, where ten consecutive time frames were summed together.
160 If the value of any of these summing events was greater or equal to seven (indicating a
161 fluorescent change of > 3 standard deviations in 7/10 time frames), a neuron was deemed to be
162 active. For THIP sleep experiments, the five minutes of inactivity occurring after an initial 30
163 seconds of behavioral inactivity were used. After identifying firing neurons for each condition
164 (wake vs sleep), the percentage of active neurons was calculated in each slice by taking the
165 number of active neurons and dividing it by the total number of neurons.
166 Traces of active neurons were used to calculate the number of firing events. This was done
167 using the 'findpeaks' matlab function on the zscored fluorescent traces, with the parameters
168 'minpeakheight' of 3, and 'minpeakdistance' of 30. Data resulting from this was crosschecked
169 by taking the binary matrices of the time traces and finding the number of times each neuron
170 met the activity threshold described above. Graph-theory analyses of neural connectivity were
171 performed as described previously [10] .
172
173 **Behavioral sleep analysis**
174 Behavioral data for flies in imaging experiments was analyzed as previously [10] using a
175 custom-written MatLab code that measured the pixel change occurring over the legs of the fly
176 on the ball over the entire time series. Data was analyzed and graphed using Graphpad Prism.
177 All data was checked for Gaussian distribution using a D'Agostino-Pearson normality test prior
178 to statistical testing. Data from THIP experiments was analyzed using a non-parametric Mann-
179 Whitney test.
180 Sleep behavior in freely-walking flies was analyzed with the Drosophila ARousal Tracking
181 system (DART) as previously described [33]. Prior to analysis, 3-5 day-old females were

collected and loaded individually into 65 mm glass tubes (Trikinetics) that were plugged at one end with standard fly food, containing either 0.1 mg/ml THIP or 0.5 mg/ml all-trans-retinal (ATR). Controls were placed onto normal food and housed under identical conditions as the experimental groups. The tubes were placed onto platforms (6 total platforms, 17 tubes per platform, up to 102 flies total) for filming. Flies were exposed to ultra-bright red LED (617 nm Luxeon Rebel LED, Luxeon Star LEDs, Ontario, Canada) which produce 0.1-0.2mW/mm2 at a distance of 4-5 cm with the aid of 723 concentrator optics (Polymer Optics 6° 15 mm Circular Beam Optic, Luxeon Star LEDs) for the duration of the experiment for optogenetic activation. Significance was determined by ANOVA with Tukey's multiple comparisons test (GraphPad Prism). Sleep analysis in nAchRα knockout animals was performed using Trikinetics beam-crossing devices, with regular (>5min) and short sleep (1-5min) calculated as previously [10].

Sleep deprivation

Flies were sleep deprived (SD) with the use of the previously described Sleep Nullifying Apparatus (SNAP), an automated sleep deprivation apparatus that has been found to keep flies awake without nonspecifically activating stress responses [34]. Vials containing no greater than 20 flies, which contained either standard food medium or medium containing 0.1mg/ml THIP were placed on the SNAP apparatus for continuous sleep deprivation. The SNAP apparatus was programmed to snap the flies once every 20 seconds for the duration of the sleep deprivation protocol.

RNA-Sequencing

Flies collected for RNA-sequencing analysis were first housed in vials containing either 0.5mg/ml all-trans retinal (ATR) or 0.1mg/ml THIP for sleep induction, along with their

genetically identical controls on standard food medium. Flies undergoing sleep induction by dFB optogenetic activation with ATR and their controls were placed under constant red-light from 8AM until 6PM to coincide with normal 12:12 light/dark cycles. Flies were collected after 1 hour (ZT 1) and 10 hours (ZT 10) post induction for immediate brain dissection and RNA extraction. For analysis of pharmacological sleep induction, flies were placed on THIP or normal food medium at 8AM (ZT 0) and collected for dissection at 6PM (ZT 10).

Whole fly brains were dissected in ice cold RNA*later (Sigma-Aldrich)* with 0.1% PBST as per previously published protocol [35]. The dissected brains were immediately pooled into five 1.5-mL Eppendorf tubes containing 5 brains (n = 25) each. Total RNA was immediately purified using TRIzol according to the manufacturer's protocols (Sigma-Aldrich) and stored at -80°C until commencement of RNA-sequencing.

cDNA libraries were prepared using the Illumina TruSeq stranded mRNA library prep kit. Image processing and sequence data extraction were performed using the standard Illumina Genome Analyzer software and CASAVA (version 1.8.2) software. Cutadapt (version 1.8.1) was used to cut the adaptor sequences as well as low quality nucleotides at both ends. When a processed read is shorter than 36 bp, the read was discarded by cutadapt, with the parameter setting of "-q 20,20 --minimum-length=36". Processed reads were aligned to the *Drosophila melanogaster* reference genome (dm6) using HISAT2 (version 2.0.5) [36], with the parameter setting of "--no-unal --fr --rna-strandness RF --known-splicesite-infile dm6_splicesites.txt". This setting is to i) suppress SAM records for reads that failed to align ("--no-unal"), ii) specify the Illumina's paired-end sequencing assay and the strand-specific information ("--fr --rna-strandness RF") and iii) provide a list of known splice sites in *Drosophila melanogaster* ("--known-splicesite-infile dm6_splicesites.txt"). Samtools (version 1.3) [37] was then used to convert "SAM" files to "BAM" files, sort and index the "BAM" files. The "htseq-count" module in the HTSeq package (v0.7.1) was used to quantitate the gene expression level by

generating a raw count table for each sample (i.e. counting reads in gene features for each sample). Based on these raw count tables, edgeR (version 3.16.5) [38] was adopted to perform the differential expression analysis between treatment groups and controls. EdgeR used a trimmed mean of M-values to compute scale factors for library size normalization [39]. It used the Cox-Reid profile-adjusted likelihood method to estimate dispersions [40] and the quasi-likelihood F-test to determine differential expression [41]. Lowly expressed genes in both groups (the mean CPM < 5 in both groups) were removed. Differentially expressed genes were identified using the following criteria: i) FDR < 0.05 and ii) fold changes > 1.5 (or logfc >0.58). Gene ontology enrichment analysis for differentially expressed genes was performed using the functional annotation tool in DAVID Bioinformatics Resources (version 6.8) [42, 43].

Gene expression

RNA and cDNA Synthesis

A quantitative reverse transcriptase PCR assay was used to confirm expression of genes enriched during THIP sleep induction. Nineteen candidate genes were selected (eight negatively and eleven positively) for the gaboxadol (THIP) sleep analysis and six genes (four negatively and two positively) for the dFSB activation experiments. Total RNA was isolated using the Directzol RNA kit (ZymoResearch) from twenty adult brains per condition and each condition was collected in triplicate. RNA quality was confirmed using a microvolume spectrophotometer NanoDrop 2000 (Thermo, USA) with only those resulting samples meeting optimal density ratios between 1.8 and 2.1 used. Up to 1 µg of total RNA was reverse transcribed using a High-Capacity cDNA Reverse Transcription Kit (Themo, USA) as per the manufacturer's protocols. The synthesis of cDNA and subsequent amplification was performed in max volumes of 20 µL per reaction using the T100 Thermal Cycler (Bio-Rad, USA). Thermocycle conditions were as such; 25 °C for 10 min, 37 °C for 120 min, 85 °C for 5 min,

and held at 4 °C . All cDNA was subsequently stored at − 20 °C until used. Target genes for THIP experiments included Pxt (CG7660, FBgn0261987), RpS5b (CG7014, FBgn0038277), Dhd (CG4193, FBgn0011761), CG9377 (CG9377, FBgn0032507), aKHr (CG11325, FBgn0025595), Acox57D-d (CG9709, FBgn0034629), FASN1 (CG3523, FBgn0283427), Pen (CG4799, FBgn0287720), CG10513 (CG10513, FBgn0039311), Gasp (CG10287, FBgn0026077), Act57B (CG10067, FBgn0000044), Bin1 (CG6046, FBgn0024491), verm (CG8756, FBgn0261341), CG16885 (CG16885, FBgn0032538), CG16884 (CG16884, FBgn0028544), CG5999 (CG5999, FBgn0038083), Fbp1 (CG17285, FBgn0000639), CG5724 (CG5724, FBgn0038082), Eh (CG5400, FBgn0000564). Target genes for dFSB experiments included Vmat (CG33528, FBgn0260964), Dop1R1 (CG9652, FBgn0011582), Salt (CG2196, FBgn0039872), Dysb (CG6856, FBgn0036819), Irk3 (CG10369, FBgn0032706), Blos1 (CG30077, FBgn0050077). Housekeeping genes included Rpl32 (CG7939, FBgn0002626), Gapdh2 (CG8893, FBgn0001092), Actin 5C (CG4027, FBgn0000042). Primer sequences can be found in Supplementary Table 8.

Quantitative real-time PCR

Quantitative (q) RT-PCR was carried out using the Luna Universal qPCR Master Mix (NEB) in the CFX384 Real-Time system (Bio-Rad, USA). Cycling conditions were: 1. 95°C for 60 s, 2. 95°C for 15s, 3. 60°C for 60s with 39 cycles of steps two and three. Melt curve analysis was then performed with the following conditions 1. 95°C for 15s, 2. 60°C for 60s, 3. 95°C for 15s. Three biological replicates for each condition as well as three technical replicates per biological sample were loaded. Each experiment was then repeated on three separate occasions. Cq values and standard curves were generated using Bio Rad CFX Manager Software to ensure amplification specificity. Results were normalized to the above housekeeping genes and gene expression was calculated following the 2^− ΔΔCq method (Livak and Schmittgen 2001).

282

283 **Gene knockouts and knockdowns**

284 Dα1KO harboured an ends-out mediated deletion of Dα1 in a w^{1118} background with the X
285 chromosome replaced with one from the wild type line DGRP line 59 [44].

286 For Dα2KO, Dα3KO, Dα4KO, Dα6KO, Dα7KO, two sgRNAs were designed to target the start
287 and the end of the coding sequence and cloned into either pU6-BbsI-gRNA or pCFD4
288 plasmids. These plasmids were then microinjected into *Drosophila* embryos to generate
289 transgenic strains stably expressing sgRNAs. These strains were crossed to another strain
290 expressing Cas9 under Actin promoter (ActinCas9). Their offspring were screened for deletion
291 events with PCR and crossed to appropriate balancer strains to isolate and generate
292 homozygous knockout strains. Full deletions were identified for all these subunit genes except
293 for Dα3 which has two partial deletions at the 3' and 5' ends [45]. ActinCas9 strain was used
294 as genetic control for Dα3KO and Dα7KO, while this same strain with the X chromosome
295 replaced with one from w^{1118} (w^{1118}ActinCas9) was used as genetic control for Dα2KO,
296 Dα4KO, and Dα6KO. RNAi strains for gene knockdown experiments (UAS-*AkhR*-RNAi)
297 were obtained from the VDRC (KK109300).

298

Results

Prolonged dFB and THIP-induced sleep have near identical effects on sleep duration

We first compared pharmacological and optogenetic sleep (**Figure 1**) by using the traditional behavioral metrics employed by most *Drosophila* sleep researchers: >5 minutes inactivity for flies confined in small glass tubes over multiple days and nights [15, 16]. We found that dFB- and THIP-induced sleep yielded almost identical effects on sleep duration, with both significantly increasing total sleep duration for both the day and night, when compared to controls (**Figure 2A-D**; **Supplementary Table 1**). An increase in total sleep duration can be due to either an increase in the number of sleep bouts that are occurring (reflective of more fragmented sleep), or an increase in the average duration of individual sleep bouts, which indicates a more consolidated sleep structure [46-48]. To investigate whether both sleep induction methods also had similar effects on sleep architecture, we plotted bout number as a function of bout duration for dFB and THIP-induced sleep, for the day and night [49]. We found that both dFB activation and THIP provision produce a similar increase in sleep consolidation during the day (**Figure 2E, F**). During the night, induced sleep effects were also similar, although less clearly different to the spontaneous sleep seen in control flies (**Figure 2G, H**). Interestingly, red light exposure decreased average night bout duration in non-ATR control flies (**Supplementary Figure 1A-D**), suggesting a light-induced artefact at night. For THIP, we observed an increase in both bout number and duration during the day, and an increase in bout duration during the night (**Supplementary Figure 1E,F**). Taken together, these results show that prolonged dFB activation and THIP provision have similar behavioral effects on induced sleep in *Drosophila*, with increases in the total amount of sleep and the level of sleep consolidation. Without any further investigations, this might suggest that both sleep induction methods represent similar underlying processes.

THIP-induced sleep decreases brain activity and connectivity

The brain presents an obvious place to look for any potential differences between sleep induction methods. In a previous study employing whole-brain calcium imaging in tethered flies we showed that optogenetic activation of the dFB promotes wake-like sleep, with neither neural activity levels nor connectivity metrics changing significantly even after 15min of dFB-induced sleep [10]. We therefore utilized the same fly strain as in that study (R23E10-Gal4>UAS-Chrimson88-tdTomato;Nsyb-LexA>LexOp-nlsGCaMP6f) to examine the effect of THIP-induced sleep on brain activity (**Figure 3A,B**). Since we were interested in comparing acute sleep induction effects on brain activity (as opposed to prolonged sleep induction effects on behavior, as in Figure 2), we adapted our calcium imaging approach to allow a brief perfusion of THIP directly onto the exposed fly brain (**Figure 3A**, see Methods). As done previously for examining dFB-induced sleep [10], we examined calcium transients in neural soma scanning across 18 optical slices of the central fly brain (**Figure 3B,** left) and identified regions of interest (ROIs) corresponding to neuronal soma in this volume (**Figure 3B**, right, and see Methods). As shown previously [10], optogenetically activating the dFB renders flies asleep without changing the average level of neural activity measured this way (**Figure 3C**). To determine the effect of THIP on neural activity in the exact same strain, we transiently perfused onto the fly brain the minimal THIP dosage required to reliably promote sleep in flies within five minutes (0.2mg/ml) [9]. In contrast to dFB-induced sleep, we observed overall decreased neural activity coincident with the flies falling asleep, and flies remained asleep well after the drug was washed out (**Figure 3D**). To ensure that we were actually putting flies (reversibly) to sleep in this preparation, we probed for behavioral responsiveness by puffing air onto the fly once every minute (50 ms duration, 10 psi) (**Figure 4A,B**). Since the time when flies fell asleep following five minutes of THIP perfusion could be variable [9], arousal probing during sleep was only initiated after 5 min of complete

quiescence (**Figure 4B**, behavioral, upper). We observed decreased arousability for flies that had been induced to sleep via THIP perfusion (**Figure 4C**). Drug-induced sleep was however reversible, with flies returning to baseline levels of behavioral responsiveness to the air puffs ~20-30 min after sleep initiation. This confirmed that the brief exposure to THIP was indeed putting flies to sleep, with an expected sleep inertia lasting the length of a typical spontaneous sleep bout [15, 16].

We then examined more closely neural activity in flies that had been put to sleep with THIP. We found that neural activity decreased rapidly within 5 min after sleep onset (**Figure 4D**, +THIP, early). Correlation analysis also revealed a decrease in connectivity among the remaining active neurons (**Figure 4E**, +THIP, early). We also analyzed the next 5 min of sleep and observed similar results (**Figure 4D,E**, +THIP, mid). All flies eventually woke up from THIP-induced sleep, and brain activity returned to wake levels in three flies that were recorded throughout (**Figure 4D**). These observations suggest that acute THIP exposure is promoting rapid entry into a 'quiet' sleep stage in flies, bypassing the wake-like sleep evident during the first 5 min of spontaneous sleep onset [10]. Importantly, THIP-induced sleep appears to be dissimilar from dFB-induced sleep in this genotype, at the level of neural activity as well as connectivity [10].

In recent work we showed that rendering flies unresponsive with a general anesthetic, isoflurane, decreases the diversity of neural activity across the fly brain, whereas dFB-induced sleep did not show any differences in ensemble dynamics [50]. We therefore questioned if THIP-induced sleep resembled this aspect of anesthesia induction. Since we were recording from neural soma that we could track through time, we were able to assess the level of overlap between the neurons that remained active during THIP-induced sleep and

wakefulness (**Figure 4F, G**). We found that ~30% of active neurons during THIP-induced sleep were also active during wake (**Figure 4G, H**). We next examined whether the same neurons remained active across successive 5min epochs during THIP-induced sleep compared to wake. We found that there is significantly more overlap between successive 5min sleep epochs (41%), compared to the waking average (**Figure 4H**), suggesting less neural turnover during THIP-induced sleep than during wake. Taken together, our calcium imaging data confirm that pharmacological sleep induction promotes a different kind of sleep than dFB sleep induction in the same strain, more closely resembling anesthesia induction. Henceforth, we call this 'quiet' sleep, in contrast to the 'active' sleep that seems to be engaged by dFB activation [2, 10]. Notably, calcium imaging of spontaneous sleep bouts in *Drosophila* also revealed active and quiet sleep stages [10], suggesting that both of our experimental approaches are physiologically relevant. Whether drug perfusion to the brain is equivalent to feeding is of course less clear. When feeding on 0.1mg/ml THIP-laced food, flies were continuously exposed to the drug over days, with comparatively less reaching the brain. With perfusion, the brain was directly exposed to 0.2mg/ml THIP for only 5 minutes. Interestingly, in both cases this induces daytime sleep bouts which average around 25min (**Supplementary Figure 1F, Figure 4C**), the average duration of a spontaneous night-time sleep bout (**Supplementary Figure 1F; Table S1**).

Transcriptional analysis of flies induced to sleep by THIP provision

Our calcium imaging experiments suggest that different biological processes might be engaged by dFB sleep compared to THIP-induced sleep. Additionally, we observed neural effects encompassing much of the fly brain (**Figure 4F**), as our recording approach exploited a pan-neural driver. We therefore wondered if either sleep-induction method might lead to differences in gene expression across the whole brain, and if these might highlight distinct

399 molecular pathways engaged by either kind of sleep. To address this, we collected brains
400 from flies that had been induced to sleep by either method, and compared the resulting
401 transcriptomes with identically handled control animals that had not been induced to sleep by
402 these methods.
403
404 To control for genetic background, we again used the same R23E10-Gal4 > UAS-Chrimson
405 flies as in our multi-day behavioral experiments and fed the flies either THIP or ATR, as in
406 **Figure 2**. We only examined daytime sleep-induction effects for either method, as this is when
407 we observed the greatest increase in sleep compared to controls (**Figure 2**), and previous work
408 has shown that daytime sleep induction using either method achieves sleep functions [10, 23].
409 We present our THIP results first. Since THIP is a GABA-acting drug that probably affects a
410 variety of processes in the brain aside from sleep, we also assessed the effect of THIP on flies
411 that were prevented from sleeping (**Figure 5A**, left panel). Sleep deprivation (SD) was
412 performed by mechanically arousing flies once every 20 seconds for the duration of the
413 experiment, on a 'SNAP' apparatus [23, 34]. RNA was extracted from the brains of all groups
414 of flies (+/- THIP, +/- SD) after 10 hours of daytime (8am-6pm) THIP (or vehicle) provision.
415 Samples for RNA-sequencing were collected in replicates of 5 to ensure accuracy, and any
416 significant transcriptional effects were thresholded at a log fold change of 0.58 (see Methods).
417
418 Flies allowed to eat food containing 0.1mg/ml THIP *ad lib* over 10 daytime hours led to 129
419 significant changes in gene expression compared to vehicle-fed controls, with the large
420 majority (110) being downregulated and only 19 upregulated (**Figure 5B,C,E;**
421 **Supplementary Table 2**). In contrast, when THIP-fed flies were prevented from sleeping
422 this led to mostly upregulated genes (88 upregulated vs 21 downregulated, **Figure 5B,D,F;**
423 **Supplementary Table 3**). Not surprisingly, preventing sleep in THIP-fed flies led to an

almost entirely non-overlapping set of gene expression changes (**Figure 5B**). This suggests that the large number of down-regulated genes in +THIP / -SD flies pertain to sleep processes, whereas the large number of upregulated genes in +THIP / +SD flies relate to waking processes, with only a few (9) potentially attributable to the common effect of ingesting THIP.

Gene Ontology analysis on genes that were downregulated as a result of THIP-induced sleep highlighted a significant enrichment of metabolism pathways (**Figure 5E,F; Supplementary Figure 2**). The top Gene Ontology biological processes included primary, organic substance, cellular, biosynthetic and nitrogen compound metabolic pathways, as well as ribosomal processes. Interestingly, these downregulated processes are largely consistent with a recently published mouse sleep transcriptome study [51]. Among the metabolism pathways uncovered in this dataset we observed over-representation of expected genes such as *bgm* (bubblegum CG4501), *Acer* (Angiotensin-converting enzyme-related CG10593). Both of these genes are found in the primary metabolic and organic substance metabolic processes as well as within the Sleep Gene Ontology dataset (GO:0030431). Another downregulated metabolic gene is AkhR (adipokinetic hormone receptor), which has been found to regulate starvation-induced sleep in *Drosophila* [52]. AkhR belongs to the Class A GPCR Neuropeptide and protein hormone receptors which are a gene class involved in storage fat mobilization, analogous to the glucagon receptor found in mammals [53].

Although THIP-induced sleep overwhelmingly led to gene downregulation, a few genes (19) were significantly upregulated. Gene Ontology analysis on these upregulated genes highlighted enrichment in varying groups including developmental processes and multicellular organismal processes (**Figure 5E,F; Supplementary Figure 2**). Some groups were enriched under the

organic substance metabolic process pathways; however, there was no overlap when comparing these to the pathways enriched due to downregulation of genes. There were some overlapping enriched pathways when we compared the gene sets from sleep-deprived flies which had also been treated with THIP (**Figure 5F**; **Supplementary Figure 3**). However, the gene sets they involve are upregulated in the SD dataset but downregulated in sleeping flies. Interestingly, the non-sleeping THIP dataset uncovered a significant enrichment of pathways involved in the response to stress. This might be expected for flies exposed to regular mechanical stimuli over 10 hours. None of these pathways featured in the THIP sleep dataset.

To validate these findings, we conducted qRT-PCR analyses on several genes (n=19) from our THIP sleep dataset and compared these results to our original transcriptional data. The genes represented a range of both up – and down-regulated genes, and we found good correspondence between the groups (**Figure 5G**), confirming our RNA sequencing results.

Transcriptional analysis of flies induced to sleep by dFB activation

We next examined the effect of dFB-induced sleep on the whole-brain transcriptome, to compare to our THIP-induced sleep data. Based on our earlier findings that showed that dFB activation results in rapidly inducible sleep behavior that consolidates over at least 12 daytime sleep hours (**Figure 2C,E,G**), as well as our previous study showing that 10 daytime hours of dFB activation corrects attention defects in sleep-deprived flies [10], we induced sleep in R23E10-Gal4 x UAS-Chrimson flies for 10 daytime hours and collected tissue for whole-brain RNA-sequencing (**Figure 6A**). We selected two time points for collection, for both the sleep-induced flies (+ATR) as well as their genetically identical controls that were not fed ATR (-ATR; **Figure 6A**). Optogenetic activation of the dFB was matched to the normal day-time light cycle (8 AM – 8 PM). The first collection point was after 1 hour (ZT1, 9 AM) of red-light

474 exposure, to control for effects of ATR provision (when compared to ZT1, -ATR controls) as
475 well as to uncover any potential short-term genetic effects of dFB activation. We then collected
476 flies after 10 hours of red-light exposure (ZT 10, 6 PM) to examine longer-term genetic effects
477 of dFB sleep induction, and to match exactly our THIP sleep collection timepoint (i.e., 10 hours
478 of induced daytime sleep by either method). The combined collection points also allowed us
479 to compare transcriptional profiles between conditions (e.g., ZT10 +ATR vs. ZT10 -ATR), to
480 identify sleep genes, as well as within conditions (ZT1 vs. ZT10), to account for genetic effects
481 potentially linked to circadian rhythms. As for the THIP sleep data in the same strain, samples
482 for RNA-sequencing were collected in replicates of 5 to ensure accuracy, and any significant
483 transcriptional effects were thresholded at a log fold change of 0.58 (see Methods).
484

485 We first examined the effect of 10 hours of daytime dFB-induced sleep. Here, we compared
486 ATR-fed R23E10-Gal4 x UAS-Chrimson flies to genetically identical animals that were also
487 exposed to red light for 10 hours but not provided with ATR in their food (ATR-). The control
488 flies were therefore never induced to sleep by dFB activation, although they were still able to
489 sleep spontaneously (see **Figure 2C,E,G**). We found that 10 hours of dFB activation led to 278
490 significant transcriptional changes, comprising mostly of upregulated genes, with 171
491 upregulated compared to 107 downregulated (**Figure 6B,C,E; Supplementary Table 4**). In
492 contrast to the THIP-induced sleep dataset, transcriptional analysis of 10hr dFB sleep induction
493 uncovered a variety of different processes predominantly related to the regulation of biological
494 and cellular processes, rather than metabolism specifically (**Figure 6E; Supplementary**
495 **Figure 4**). For example, of the genes that were overexpressed there is an enrichment of the
496 Semaphorin-plexin signaling pathway (GO:0071526, GO:1902287, GO:1902285 and
497 GO:2000305) and the ephrin receptor signaling pathway (GO:0046011), both of which are
498 known to be involved in axonal guidance (**Figure 6F**). Interestingly, several upregulated genes

code for different subunits of nicotinic acetylcholine receptors (nAchRα1,3,4 &5). Importantly, there was almost no overlap with our sleep deprivation dataset (**Supplementary Table 3**), ruling out the possibility that optogenetic activation of the dFB is simply paralyzing awake flies and therefore causing stress (only one upregulated gene was shared, CG40198). Of the genes that were downregulated there is enrichment of pathways that relate to synaptic vesicle recycling (GO:0036465 and GO:0036466) as well as neurotransmitter metabolic processes (GO:0042133) (**Figure 6F; Supplementary Figure 4**).

In contrast to the 10hr timepoint, 1 hr of dFB sleep had far fewer transcriptomic consequences, with only 17 genes upregulated and 10 downregulated (**Figure 6B,D**). This small number of transcriptomic changes (see **Supplementary Table 5**) may reflect the effect of ATR feeding, rather than any genes relevant to dFB sleep. That 9 hours of additional dFB sleep increased transcriptomic changes by an order of magnitude lends confidence to the interpretation that relevant genes linked to prolonged dFB activation are being engaged.

To account for potential genetic effects linked to circadian expression cycles, we compared transcriptional profiles between 10 hours of induced dFB sleep to 1 hour of induced dFB sleep. Here, we found 220 differentially regulated genes (119 upregulated and 101 downregulated) when comparing ATR-fed flies at both time points (ZT10 vs ZT1, **Supplementary Table 6**). Since the 1-hour group was collected in the morning and the 10-hour group was collected in the evening, we expected this dataset to expose a number of circadian-regulatory genes, and this is indeed what we found (**Supplementary Figure 5A,B**). We then compared these results with a parallel ZT10 vs ZT1 experiment where flies were not fed ATR. Here we uncovered

503 differentially expressed genes (252 upregulated and 251 downregulated) when comparing flies that had not been fed ATR at both timepoints (**Supplementary Table 7**). Importantly, there were 98 genes that overlapped between these independent Z10 vs ZT1 datasets, suggesting commonalities linked to circadian processes. Indeed, GO Pathway analysis of Biological Processes revealed a number of genes involved in the regulation of the circadian rhythm among these 98 overlapping genes, including the well-known circadian genes *period, timeless, clockwork-orange, clock and vrille*. Notably, co-factors *period* and *timeless* are both upregulated whereas *clk* is downregulated, and this is replicated in both independent datasets (**Supplementary Figure 5C**). This correspondence with expectations for circadian effects provides a level of confidence that our respective sleep datasets are highlighting transcriptomic changes and biological pathways relevant to either sleep induction approach. Notably, there was no overlap at all in gene expression changes between dFB-induced sleep and THIP-induced sleep (**Supplementary Tables 2 & 4**), and the respective GO pathways analyses of biological processes are also largely non-overlapping (**Supplementary Figure 6**).

To validate these findings, we compared our transcriptional results with qRT-PCR on six genes. This included the dopamine receptor Dop1R1, which regulates arousal levels [55] as well as the schizophrenia susceptibility gene dysbindin (*Dysb*), which has been shown to regulate dopaminergic function [56]. We found good correspondence between our qRT-PCR data and our transcriptomic data (**Figure 6G**), confirming our RNA sequencing results.

Nicotinic acetylcholine receptors regulate sleep architecture

While THIP-induced sleep caused a systemic downregulation of metabolism-related genes,

the effect of dFB-induced sleep on gene expression was less clear. This may be consistent with our earlier observation that brain activity looks similar to wake during dFB-induced sleep [10], so we could essentially be highlighting biological processes relevant to an awake fly brain, such as dopamine function [57]. However, optogenetic activation of the dFB is not like wake, in that flies are rendered highly unresponsive to external stimuli, so perhaps like REM sleep in mammals a different category of molecular processes could be involved. In mammals, acetylcholine generally promotes wakefulness and alertness, but activity of cholinergic neurons is also high during REM sleep [58]. Neurotransmission in the insect brain is largely cholinergic, with 7 different nicotinic 'alpha' receptor subunits [59]. Interestingly, four of these subunits were upregulated in our dFB sleep dataset: nAchRα1, nAchRα3, nAchRα4, and nAchRα5. For comparison, none of these were upregulated in our sleep deprivation dataset, suggesting a sleep-relevant role. Previous studies have demonstrated a role for some of these same receptor subunits in sleep regulation, in particular nAchRα4 (also called *redeye*) which is upregulated in short-sleeping mutants [60] and nAchRα3 which has been reported to regulates arousal levels in flies [61]. Together, these studies suggest processes that might be reconsidered in the context of active sleep, as highlighted by our transcriptomic findings. We therefore sought to examine the role of cholinergic signalling in sleep more closely, by knocking out all nAchRα subunits and examining effects of each subunit knockout on sleep architecture. Since our transcriptomic analysis encompassed effects of active sleep on whole-brain gene expression, we knocked out each nAchRα subunit across the brain, by testing confirmed genetic deletions [45, 62].

We first examined the effect of each nAchRα subunit deletion on sleep duration, using the 5 minute criterion for quantifying sleep in *Drosophila* [15]. We found that the nAchRα mutants fell into two different categories: nAchRα1 and nAchRα2 significantly decreased sleep, day

569 and night; whereas nAchRα3, nAchRα4, nAchRα6 and nAchRα7 significantly increased
570 sleep, day and night (**Figure 7A**). The nAchRα5 knockout is homozygous lethal, so was not
571 included in our sleep analyses. To examine sleep architecture in these mutants, we quantified
572 sleep bout number and duration and plotted these together as done previously for our sleep
573 induction experiments (**Figure 2**). Examining the data this way, it is clear to see how
574 nAchRα1 and nAchRα2 are different: most sleep bouts are very short, day and night (**Figure**
575 **7B**, top 2 rows, left panels, green dots). In contrast, knocking out the other alpha subunits
576 seems to consolidate sleep, especially at night (**Figure 7B**, bottom 4 rows, left panels).
577 nAchRα3 was most striking in this regard, with these flies sleeping uninterrupted for an
578 average of 156.53 minutes (± 18.06) during the day and 160.76 minutes (± 17.92) at night.
579 Increased sleep consolidation in these mutants was however not due to lack of activity. While
580 awake, nAchRα3 animals were just as active as controls (activity per waking minute = 2.69 ±
581 0.18 versus 2.5 ± 0.06, respectively).

582 We next questioned what kind of sleep the nAchRα knockout flies might be getting. In
583 previous work we have shown that flies can be asleep already after the first minute of
584 inactivity, and that during the first five minutes of sleep the fly brain displays wake-like
585 levels of neural activity [10]. We have termed this early sleep stage 'active sleep' to
586 distinguish it from 'quiet sleep' that typically follows after 5-10 minutes [63]. One way of
587 estimating the amount of 'active sleep' in *Drosophila* flies is to sum all short sleep epochs
588 lasting between 1-5 minutes and expressing this as a percentage of total sleep [10]. When we
589 re-examined our nAchRα knockouts in this way, we found that this behavioral readout for
590 'active sleep' was significantly affected by the loss of select nAchRα subunits. Short sleep
591 increased significantly during both the day and the night in nAchRα1 and nAchRα2 (**Figure**
592 **7B**, top 2 rows, right panel, green dots). In contrast, and consistent with our sleep architecture

analyses (above), nAchRα3 displayed almost no short sleep (**Figure 7B**, row 3, right panel). Finally, in nAchRα4 and nAchRα6 short sleep was significantly decreased at night, while in nAchRα7 short sleep was significantly decreased day and night (**Figure 7B**, rows 4-6, right panel). In conclusion, every one of the nAchRα knockouts we tested affect short sleep in some way, either increasing (nAchRα1 and nAchRα2) or decreasing it (nAchRα3, nAchRα4, nAchRα6, nAchRα7).

We questioned whether these systemic effects of nicotinic receptors on short sleep were perhaps a trivial consequence of altered >5min sleep duration in these mutants, especially regarding the striking differences between nAchRα1&2 and the other subunit knockouts. We therefore returned to our 'quiet' sleep (THIP) dataset to contrast a gene derived from that study. We had found that several of the THIP-induced sleep genes are involved in metabolic processes, which are mostly downregulated (**Supplementary Table 2**). This included the adipokinetic hormone receptor (AkhR), which has previously been associated with sleep regulation [52]. We employed an RNAi strategy to downregulate this metabolic gene's expression across the fly brain in AkhR-RNAi / R57C10-Gal4 flies (see Methods). We found that downregulating AkhR significantly decreased sleep duration during the day as well as night, compared to genetic control strains (**Figure 8A,B**). Accordingly, sleep bout duration and number decreased, especially during the day (**Figure 8C**). However, in contrast to knocking out nAchRα1 and nAchRα2, which also significantly decreased sleep duration day and night, short sleep was not significantly altered in AkhR knockdown animals compared to genetic controls (**Figure 8D**). This suggests that short (1-5min) sleep might be under separate regulatory control than >5min sleep.

Discussion

One of the key advantages of studying sleep in *Drosophila* is that this versatile model provides a variety of reliable approaches for inducing and controlling sleep. By being able to induce sleep on demand, either genetically or pharmacologically, researchers have been able to manipulate sleep as an experimental variable, and in this way be better able to assess causality when probing potential sleep functions. However, this approach has often sidestepped the question of whether different sleep induction methods are equivalent, or whether distinct forms of sleep might be engaged by different genetic or pharmacological treatments. In mammals, GABA agonists typically promote slow-wave sleep (SWS), which has been associated with cellular homeostasis and repair process in the brain [4, 64]. In contrast, drugs targeting acetylcholine receptors, such as carbachol, have been found to promote brain states more reminiscent of REM sleep [65, 66]. Although these drugs all induce sedative (or dissociative) states, they are clearly producing dissimilar forms of sleep in mammals, with likely different functions or consequences for the brain. In *Drosophila*, evidence suggests that the GABA agonist THIP promotes a form of deep or 'quiet' sleep, which may be functionally analogous to mammalian SWS [9, 26, 67]. In contrast, optogenetic activation of the dFB may promote a form of active sleep, which we have suggested could be an evolutionary antecedent of REM sleep [2]. THIP-induced sleep in flies has been associated with waste clearance from the brain [26], just as SWS has been associated with clearance of waste metabolites via the mammalian brain's glymphatic system [64]. Such functional homology suggests that the transcriptional changes we uncovered for THIP-induced sleep in *Drosophila* might also be relevant for mammalian SWS, with these largely centered on reduced metabolic processes and stress regulation [51]. In contrast, except for the upregulation of cholinergic signaling [68], there is little to compare to test hypotheses potentially linking active sleep in flies with REM sleep in mammals, except for

641 the potential upregulation of cholinergic signaling. Even this cholinergic connection seems
642 odd, seeing that the predominant excitatory neurotransmitters are reversed in the brains of
643 insects and mammals: glutamate in mammals and acetylcholine in insects [69]. Additionally,
644 only nicotinic receptor subunits were identified in our analyses, whereas muscarinic receptors
645 have been more commonly associated with REM sleep in mammals [70, 71]. Nevertheless, it
646 is clear from our results that dFB-induced active sleep upregulates the expression of multiple
647 nicotinic acetylcholine subunits, and that knocking these out individually has profound (and
648 opposing) effects on sleep architecture in flies. This supports other studies showing the same
649 [60, 61], although not in relation to active sleep processes as we show here. It will be
650 especially interesting in future brain imaging studies to see whether a knockout such as
651 nAchRα3 is eliminating one kind of sleep (e.g., active sleep) as predicted by our behavioral
652 data, and whether this is associated with any functional consequences. Similarly, it will be
653 telling to see whether the opposite sleep phenotypes observed in nAchRα1 for example result
654 in a distinct class of functional consequences. A previous study has shown that nAchRα1
655 knockout animals have significantly shorter survivorship compared to controls, with flies
656 dying almost 20 days earlier [44]. One reason could be because of impaired or insufficient
657 deep sleep functions (e.g., brain waste clearance [26]). The nAchRα knockouts provide an
658 opportunity to further examine mutant animals potentially lacking either kind of sleep,
659 although this will have to be confirmed by brain imaging or electrophysiology.

660 We found little similarity between two different approaches to inducing sleep in flies, at the
661 level of gene expression as well as brain activity. It may however not be surprising that these
662 entirely different sleep induction methods produce dissimilar physiological effects. After all,
663 one method requires flies to ingest a drug which then must make its way to the brain, while
664 the other method acutely activates a subset of neurons in the central brain. Yet both methods
665 yield similarly increased sleep duration profiles and consolidated sleep architecture (**Figure**

2). One underlying assumption with focusing on sleep duration as the most relevant metric for understanding sleep function in *Drosophila* is that sleep is a unitary phenomenon in the fly model, meaning that primarily one set of functions and one form of brain activity are occurring when flies sleep. There is now substantial evidence that this is unlikely to be true, and that like other animals flies probably also experience distinct sleep stages that accomplish different functions [9, 10, 26, 63, 72, 73]. This does not mean that these functions are mutually exclusive; for example, both THIP provision and dFB activation have been found to promote memory consolidation in *Drosophila* [23]. Indeed, it seems reasonable to propose that different sleep stages could be synergistic, accomplishing a variety of homeostatic functions that might be required for adaptive behaviors in an animal. Our results suggest that THIP provision promotes a 'quiet sleep' stage in flies, which induces a brain-wide downregulation of metabolism-related genes. This is consistent with studies in flies showing that metabolic rate is decreased in longer sleep bouts, especially at night, and that this is recapitulated by THIP-induced sleep [74]. One argument for why metabolism-related genes are downregulated during THIP-induced sleep might be that flies are starved (because they are sleeping more). However, flies induced to sleep by dFB activation are also sleeping more, and these did not reveal a similar downregulation of metabolic processes. Another view might be that our sampling was done after flies had achieved 10 hours of induced sleep, so sleep functions might have already been achieved by that time. Thus, we might not be uncovering genes required for achieving 'quiet' sleep functions as much as identifying exactly the opposite: genetic pathways that have been satisfied by 10 hours of induced quiet sleep. Other studies using THIP to induce sleep have examined longer timeframe (e.g., 2 days {Dissel, 2015 #493}), so it remains unclear whether changes in gene regulation relate to sleep functions that have been achieved or that are still being engaged. Our key result is that none

690 of these genes are shared by flies collected after exactly the same duration of dFB-induced
691 sleep.

692 In contrast to THIP, optogenetic dFB activation promotes an 'active sleep' stage which
693 induces a brain-wide upregulation of a variety of neural mechanisms, including cholinergic
694 subunit receptors. Although many studies have shown that the R23E10-Gal4 circuit is sleep
695 promoting (e.g.[19, 21, 73]), it seems unlikely that active sleep regulation is limited to these
696 specific dFB neurons alone [75]. Other circuits in the fly central brain are also sleep-
697 promoting, including in the ellipsoid body [76] and the ventral fan-shaped body (vFB) [77],
698 although it remains unknown if activation of these other circuits also promotes an active
699 sleep stage, or whether a similar transcriptome might be engaged by these alternate
700 approaches to optogenetic sleep induction in flies. This again highlights a variant of the same
701 problem we have uncovered in the current study comparing pharmacology with optogenetics:
702 different circuit-based approaches could all be increasing sleep duration but achieving
703 entirely different functions by engaging distinct transcriptomes and thus different sleep
704 functions. How many different kinds of functions are engaged by sleep remains unclear: is it
705 roughly two functional categories linked to quiet and active sleep, or is it a broader range of
706 sub-categories that are not so tightly linked to these obviously different brain activity states?

707

708 A compelling argument could nevertheless be made for two kinds of sleep in most animals,
709 with two distinct sets of functions [1, 67]. Most animals have been shown to require a form of
710 'quiet' sleep to ensure survival, suggesting that these might encompass an evolutionarily
711 conserved set of cellular processes that promote neural health and development [78], and that
712 operate best during periods of behavioral quiescence. Nematode worms thus experience a
713 form of quiet sleep when they pause to molt ('lethargus') into a different life stages during
714 their development [79], or when cellular repair processes are needed following environmental

715 stress [80]. In flies, quiet sleep seems to be similarly required for neuronal repair [25] or
716 waste clearance [26], and there is evidence that glia might play a key role in these cellular
717 homeostatic processes in flies [25] as well as other animals [81]. Thus, SWS in mammals and
718 birds might present a narrow neocortical view of a more ancient set of sleep functions
719 centered on quiescence and decreased metabolic rate. Indeed, neural quiescence is also a
720 feature of SWS, both at the level of pulsed inhibition (down-states), as well as in other parts
721 of the brain beyond the cortex [1]. Similar to findings in flies that are induced into a quiet
722 sleep stage with THIP [74], metabolic rate also decreases during SWS in mammals [82]. In
723 contrast, metabolic rate is similar to waking during REM sleep in mammals [83], suggesting
724 an alternate set of functions not linked to cellular homeostasis. What might these functions
725 be, and could some of these be conserved between active sleep in invertebrates and REM
726 sleep in mammals? A REM-like sleep stage has now been identified in a variety of
727 invertebrate species, including cephalopods [12] and jumping spiders [84], while flies show
728 evidence of an active sleep stage [10]. In humans, REM sleep has been implicated in emotion
729 regulation [85], and cognitive disorders where emotions are dysregulated, such as depression,
730 are often associated with REM sleep dysfunction [86]. While it is not evident how to study
731 emotions in insects (but see [87]), it could be argued that arousal systems more generally are
732 employed to detect prediction errors and thereby promote learning [88]. Thus, we and others
733 have suggested that active sleep might be crucial for optimizing prediction, and attention, and
734 learning [2, 67, 89], and this may involve different kinds of homeostatic mechanisms
735 centered on brain circuits rather than cells. Our finding that dFB-induced active sleep in
736 *Drosophila* upregulates different nAchRα subunits is consistent with new findings that these
737 subunits regulate appetitive memories in flies [90] and that cholinergic systems more
738 generally underpin learning and memory in this animal [91]. Yet learning and memory in
739 flies also benefits from quiet sleep, as evidenced by multiple studies using THIP as a sleep-

promoting agent [23, 24, 92]. One view consistent with our findings and previous studies is that both kinds of sleep are crucial for optimal behavior: quiet sleep for cellular homeostasis and active sleep for circuit homeostasis. Manipulating these separately, alongside the non-overlapping pathways engaged by either kind of sleep, should help further disambiguate the functions potentially associated with these distinct sleep stages.

Author contributions: Designed experiments, collected and analyzed data: NA, LALT-H, HL, EN. Designed experiments and analyzed data: QZ. Designed experiments: TP, PB, PJS. Designed experiments, analyzed data, and wrote the paper: BvS.

Acknowledgements: This work was supported by National Health and Medical Research Council grant GNT1164499 to BvS and NIH R01 grant NS076980 to PJS and BvS.

Declaration of Interests: The authors declare no conflicts of interest.

References

1. Jaggard, J.B., G.X. Wang, and P. Mourrain, *Non-REM and REM/paradoxical sleep dynamics across phylogeny.* Curr Opin Neurobiol, 2021. **71**: p. 44-51.
2. Van De Poll, M.N. and B. van Swinderen, *Balancing Prediction and Surprise: A Role for Active Sleep at the Dawn of Consciousness?* Front Syst Neurosci, 2021. **15**: p. 768762.
3. Dijk, D.J., D.P. Brunner, and A.A. Borbely, *Time course of EEG power density during long sleep in humans.* Am J Physiol, 1990. **258**(3 Pt 2): p. R650-61.
4. Tononi, G. and C. Cirelli, *Sleep and the price of plasticity: from synaptic and cellular homeostasis to memory consolidation and integration.* Neuron, 2014. **81**(1): p. 12-34.
5. Siegel, J.M., *REM sleep: a biological and psychological paradox.* Sleep Med Rev, 2011. **15**(3): p. 139-42.
6. Shein-Idelson, M., et al., *Slow waves, sharp waves, ripples, and REM in sleeping dragons.* Science, 2016. **352**(6285): p. 590-5.
7. Rattenborg, N.C., et al., *Local Aspects of Avian Non-REM and REM Sleep.* Front Neurosci, 2019. **13**: p. 567.
8. Libourel, P.A. and A. Herrel, *Sleep in amphibians and reptiles: a review and a preliminary analysis of evolutionary patterns.* Biol Rev Camb Philos Soc, 2016. **91**(3): p. 833-66.
9. Yap, M.H.W., et al., *Oscillatory brain activity in spontaneous and induced sleep stages in flies.* Nat Commun, 2017. **8**(1): p. 1815.
10. Tainton-Heap, L.A.L., et al., *A Paradoxical Kind of Sleep in Drosophila melanogaster.* Curr Biol, 2021. **31**(3): p. 578-590 e6.
11. Leung, L.C., et al., *Neural signatures of sleep in zebrafish.* Nature, 2019. **571**(7764): p. 198-204.

781 12. Iglesias, T.L., et al., *Cyclic nature of the REM sleep-like state in the cuttlefish Sepia*
782 *officinalis.* J Exp Biol, 2019. **222**(Pt 1).
783 13. Sauer, S., et al., *The dynamics of sleep-like behaviour in honey bees.* J Comp Physiol
784 A Neuroethol Sens Neural Behav Physiol, 2003. **189**(8): p. 599-607.
785 14. Calcagno, B., et al., *Transient activation of dopaminergic neurons during*
786 *development modulates visual responsiveness, locomotion and brain activity in a*
787 *dopamine ontogeny model of schizophrenia.* Transl Psychiatry, 2013. **2**: p. e2026.
788 15. Shaw, P.J., et al., *Correlates of sleep and waking in Drosophila melanogaster.*
789 Science, 2000. **287**(5459): p. 1834-7.
790 16. Hendricks, J.C., et al., *Rest in Drosophila is a sleep-like state.* Neuron, 2000. **25**(1): p.
791 129-38.
792 17. Shafer, O.T. and A.C. Keene, *The Regulation of Drosophila Sleep.* Curr Biol, 2021.
793 **31**(1): p. R38-R49.
794 18. Wolff, T. and G.M. Rubin, *Neuroarchitecture of the Drosophila central complex: A*
795 *catalog of nodulus and asymmetrical body neurons and a revision of the*
796 *protocerebral bridge catalog.* J Comp Neurol, 2018. **526**(16): p. 2585-2611.
797 19. Troup, M., et al., *Acute control of the sleep switch in Drosophila reveals a role for*
798 *gap junctions in regulating behavioral responsiveness.* Elife, 2018. **7**.
799 20. Donlea, J.M., et al., *Inducing sleep by remote control facilitates memory*
800 *consolidation in Drosophila.* Science, 2011. **332**(6037): p. 1571-6.
801 21. Donlea, J.M., D. Pimentel, and G. Miesenbock, *Neuronal machinery of sleep*
802 *homeostasis in Drosophila.* Neuron, 2014. **81**(4): p. 860-72.
803 22. Donlea, J.M., et al., *Recurrent Circuitry for Balancing Sleep Need and Sleep.* Neuron,
804 2018. **97**(2): p. 378-389 e4.

805 23. Dissel, S., et al., *Sleep restores behavioral plasticity to Drosophila mutants.* Curr
806 Biol, 2015. **25**(10): p. 1270-81.
807 24. Berry, J.A., et al., *Sleep Facilitates Memory by Blocking Dopamine Neuron-Mediated*
808 *Forgetting.* Cell, 2015. **161**(7): p. 1656-67.
809 25. Stanhope, B.A., et al., *Sleep Regulates Glial Plasticity and Expression of the*
810 *Engulfment Receptor Draper Following Neural Injury.* Curr Biol, 2020. **30**(6): p.
811 1092-1101 e3.
812 26. van Alphen, B., et al., *A deep sleep stage in Drosophila with a functional role in*
813 *waste clearance.* Sci Adv, 2021. **7**(4).
814 27. Lundahl, J., et al., *EEG spectral power density profiles during NREM sleep for*
815 *gaboxadol and zolpidem in patients with primary insomnia.* J Psychopharmacol,
816 2012. **26**(8): p. 1081-7.
817 28. Mitler, M.M. and W.C. Dement, *Cataplectic-like behavior in cats after micro-*
818 *injections of carbachol in pontine reticular formation.* Brain Res, 1974. **68**(2): p. 335-
819 43.
820 29. Jenett, A., et al., *A GAL4-driver line resource for Drosophila neurobiology.* Cell Rep,
821 2012. **2**(4): p. 991-1001.
822 30. Klapoetke, N.C., et al., *Independent optical excitation of distinct neural populations.*
823 Nat Methods, 2014. **11**(3): p. 338-46.
824 31. Pfeiffer, B.D., J.W. Truman, and G.M. Rubin, *Using translational enhancers to*
825 *increase transgene expression in Drosophila.* Proc Natl Acad Sci U S A, 2012.
826 **109**(17): p. 6626-31.
827 32. Legland, D., I. Arganda-Carreras, and P. Andrey, *MorphoLibJ: integrated library and*
828 *plugins for mathematical morphology with ImageJ.* Bioinformatics, 2016. **32**(22): p.
829 3532-3534.

830 33. Faville, R., et al., *How deeply does your mutant sleep? Probing arousal to better*
831 *understand sleep defects in Drosophila.* Scientific Reports, 2015. **5**: p. 8454.
832 34. Seugnet, L., et al., *Persistent short-term memory defects following sleep deprivation*
833 *in a drosophila model of Parkinson disease.* Sleep, 2009. **32**(8): p. 984-92.
834 35. Chen, C., et al., *Drosophila Ionotropic Receptor 25a mediates circadian clock*
835 *resetting by temperature.* Nature, 2015. **527**(7579): p. 516-20.
836 36. Kim, D., B. Langmead, and S.L. Salzberg, *HISAT: a fast spliced aligner with low*
837 *memory requirements.* Nat Methods, 2015. **12**(4): p. 357-60.
838 37. Li, H., et al., *The Sequence Alignment/Map format and SAMtools.* Bioinformatics,
839 2009. **25**(16): p. 2078-9.
840 38. Robinson, M.D., D.J. McCarthy, and G.K. Smyth, *edgeR: a Bioconductor package*
841 *for differential expression analysis of digital gene expression data.* Bioinformatics,
842 2010. **26**(1): p. 139-40.
843 39. Robinson, M.D. and A. Oshlack, *A scaling normalization method for differential*
844 *expression analysis of RNA-seq data.* Genome Biol, 2010. **11**(3): p. R25.
845 40. McCarthy, D.J., Y. Chen, and G.K. Smyth, *Differential expression analysis of*
846 *multifactor RNA-Seq experiments with respect to biological variation.* Nucleic Acids
847 Res, 2012. **40**(10): p. 4288-97.
848 41. Lun, A.T., Y. Chen, and G.K. Smyth, *It's DE-licious: A Recipe for Differential*
849 *Expression Analyses of RNA-seq Experiments Using Quasi-Likelihood Methods in*
850 *edgeR.* Methods Mol Biol, 2016. **1418**: p. 391-416.
851 42. Huang da, W., B.T. Sherman, and R.A. Lempicki, *Bioinformatics enrichment tools:*
852 *paths toward the comprehensive functional analysis of large gene lists.* Nucleic Acids
853 Res, 2009. **37**(1): p. 1-13.

854 43. Huang da, W., B.T. Sherman, and R.A. Lempicki, *Systematic and integrative analysis*
855 *of large gene lists using DAVID bioinformatics resources.* Nat Protoc, 2009. **4**(1): p.
856 44-57.
857 44. Somers, J., et al., *Pleiotropic Effects of Loss of the Dalpha1 Subunit in Drosophila*
858 *melanogaster: Implications for Insecticide Resistance.* Genetics, 2017. **205**(1): p. 263-
859 271.
860 45. Perry, T., et al., *Role of nicotinic acetylcholine receptor subunits in the mode of action*
861 *of neonicotinoid, sulfoximine and spinosyn insecticides in Drosophila melanogaster.*
862 Insect Biochem Mol Biol, 2021. **131**: p. 103547.
863 46. Zimmerman, J.E., et al., *A video method to study Drosophila sleep.* Sleep, 2008.
864 **31**(11): p. 1587-98.
865 47. Huber, R., et al., *Sleep homeostasis in Drosophila melanogaster.* Sleep, 2004. **27**(4):
866 p. 628-39.
867 48. Andretic, R. and P.J. Shaw, *Essentials of sleep recordings in Drosophila: moving*
868 *beyond sleep time.* Methods Enzymol, 2005. **393**: p. 759-72.
869 49. Kirszenblat, L., R. Yaun, and B. van Swinderen, *Visual experience drives sleep need*
870 *in Drosophila.* Sleep, 2019. **42**(7).
871 50. Troup, M.J., L.A.L. Tainton-Heap, and B. van Swinderen, *Neural ensemble*
872 *fragmentation in the anesthetized Drosophila brain.* J Neurosci, 2023.
873 51. Muheim, C.M., et al., *Dynamic- and Frequency-Specific Regulation of Sleep*
874 *Oscillations by Cortical Potassium Channels.* Curr Biol, 2019. **29**(18): p. 2983-2992
875 e3.
876 52. He, Q., et al., *AKH-FOXO pathway regulates starvation-induced sleep loss through*
877 *remodeling of the small ventral lateral neuron dorsal projections.* PLoS Genet, 2020.
878 **16**(10): p. e1009181.

879 53. Bharucha, K.N., P. Tarr, and S.L. Zipursky, *A glucagon-like endocrine pathway in*
880 *Drosophila modulates both lipid and carbohydrate homeostasis.* J Exp Biol, 2008.
881 **211**(Pt 19): p. 3103-10.
882 54. Bellesi, M., et al., *Effects of sleep and wake on astrocytes: clues from molecular and*
883 *ultrastructural studies.* BMC Biol, 2015. **13**: p. 66.
884 55. Ferguson, L., et al., *Transient Dysregulation of Dopamine Signaling in a Developing*
885 *Drosophila Arousal Circuit Permanently Impairs Behavioral Responsiveness in*
886 *Adults.* Front Psychiatry, 2017. **8**: p. 22.
887 56. Shao, L., et al., *Schizophrenia susceptibility gene dysbindin regulates glutamatergic*
888 *and dopaminergic functions via distinctive mechanisms in Drosophila.* Proc Natl
889 Acad Sci U S A, 2011. **108**(46): p. 18831-6.
890 57. Van Swinderen, B. and R. Andretic, *Dopamine in Drosophila: setting arousal*
891 *thresholds in a miniature brain.* Proc Biol Sci, 2011. **278**(1707): p. 906-13.
892 58. Watson, C.J., H.A. Baghdoyan, and R. Lydic, *Neuropharmacology of Sleep and*
893 *Wakefulness.* Sleep Med Clin, 2010. **5**(4): p. 513-528.
894 59. Rosenthal, J.S. and Q. Yuan, *Constructing and Tuning Excitatory Cholinergic*
895 *Synapses: The Multifaceted Functions of Nicotinic Acetylcholine Receptors in*
896 *Drosophila Neural Development and Physiology.* Front Cell Neurosci, 2021. **15**: p.
897 720560.
898 60. Shi, M., et al., *Identification of Redeye, a new sleep-regulating protein whose*
899 *expression is modulated by sleep amount.* Elife, 2014. **3**: p. e01473.
900 61. Dai, X., et al., *Molecular resolution of a behavioral paradox: sleep and arousal are*
901 *regulated by distinct acetylcholine receptors in different neuronal types in*
902 *Drosophila.* Sleep, 2021. **44**(7).

62. Chen, W., et al., *Dual nicotinic acetylcholine receptor subunit gene knockouts reveal limits to functional redundancy.* Pestic Biochem Physiol, 2022. **184**: p. 105118.

63. van Alphen, B., et al., *A dynamic deep sleep stage in Drosophila.* J Neurosci, 2013. **33**(16): p. 6917-27.

64. Xie, L., et al., *Sleep drives metabolite clearance from the adult brain.* Science, 2013. **342**(6156): p. 373-7.

65. Kubin, L., *Carbachol models of REM sleep: recent developments and new directions.* Arch Ital Biol, 2001. **139**(1-2): p. 147-68.

66. Torterolo, P., et al., *Neocortical 40 Hz oscillations during carbachol-induced rapid eye movement sleep and cataplexy.* Eur J Neurosci, 2016. **43**(4): p. 580-9.

67. Kirszenblat, L. and B. van Swinderen, *The Yin and Yang of Sleep and Attention.* Trends Neurosci, 2015. **38**(12): p. 776-86.

68. Vazquez, J. and H.A. Baghdoyan, *Basal forebrain acetylcholine release during REM sleep is significantly greater than during waking.* Am J Physiol Regul Integr Comp Physiol, 2001. **280**(2): p. R598-601.

69. Smarandache-Wellmann, C.R., *Arthropod neurons and nervous system.* Curr Biol, 2016. **26**(20): p. R960-R965.

70. Bourgin, P., et al., *Induction of rapid eye movement sleep by carbachol infusion into the pontine reticular formation in the rat.* Neuroreport, 1995. **6**(3): p. 532-6.

71. Kashiwagi, M. and Y. Hayashi, *Life Without Dreams: Muscarinic Receptors Are Required to Regulate REM Sleep in Mice.* Cell Rep, 2018. **24**(9): p. 2211-2212.

72. Wiggin, T.D., et al., *Covert sleep-related biological processes are revealed by probabilistic analysis in Drosophila.* Proc Natl Acad Sci U S A, 2020. **117**(18): p. 10024-10034.

927 73. Gong, N.N., et al., *Intrinsic maturation of sleep output neurons regulates sleep*
928 *ontogeny in Drosophila.* Curr Biol, 2022. **32**(18): p. 4025-4039 e3.
929 74. Stahl, B.A., et al., *Sleep-Dependent Modulation of Metabolic Rate in Drosophila.*
930 Sleep, 2017. **40**(8).
931 75. Jones, J.D., et al., *Regulation of sleep by cholinergic neurons located outside the*
932 *central brain in Drosophila.* PLoS Biol, 2023. **21**(3): p. e3002012.
933 76. Liu, S., et al., *Sleep Drive Is Encoded by Neural Plastic Changes in a Dedicated*
934 *Circuit.* Cell, 2016. **165**(6): p. 1347-1360.
935 77. Lei, Z., K. Henderson, and K. Keleman, *A neural circuit linking learning and sleep in*
936 *Drosophila long-term memory.* Nat Commun, 2022. **13**(1): p. 609.
937 78. Zimmerman, J.E., et al., *Conservation of sleep: insights from non-mammalian model*
938 *systems.* Trends Neurosci, 2008. **31**(7): p. 371-6.
939 79. Raizen, D.M., et al., *Lethargus is a Caenorhabditis elegans sleep-like state.* Nature,
940 2008. **451**(7178): p. 569-72.
941 80. Hill, A.J., et al., *Cellular stress induces a protective sleep-like state in C. elegans.*
942 Curr Biol, 2014. **24**(20): p. 2399-405.
943 81. Artiushin, G. and A. Sehgal, *The Glial Perspective on Sleep and Circadian Rhythms.*
944 Annu Rev Neurosci, 2020. **43**: p. 119-140.
945 82. Caron, A.M. and R. Stephenson, *Energy expenditure is affected by rate of*
946 *accumulation of sleep deficit in rats.* Sleep, 2010. **33**(9): p. 1226-35.
947 83. Maquet, P., *Sleep function(s) and cerebral metabolism.* Behav Brain Res, 1995. **69**(1-
948 2): p. 75-83.
949 84. Rossler, D.C., et al., *Regularly occurring bouts of retinal movements suggest an REM*
950 *sleep-like state in jumping spiders.* Proc Natl Acad Sci U S A, 2022. **119**(33): p.
951 e2204754119.

952 85. Hutchison, I.C. and S. Rathore, *The role of REM sleep theta activity in emotional*
953 *memory.* Front Psychol, 2015. **6**: p. 1439.
954 86. Harrington, M.O., et al., *The influence of REM sleep and SWS on emotional memory*
955 *consolidation in participants reporting depressive symptoms.* Cortex, 2018. **99**: p.
956 281-295.
957 87. Anderson, D.J. and R. Adolphs, *A framework for studying emotions across species.*
958 Cell, 2014. **157**(1): p. 187-200.
959 88. Seth, A.K. and K.J. Friston, *Active interoceptive inference and the emotional brain.*
960 Philos Trans R Soc Lond B Biol Sci, 2016. **371**(1708).
961 89. Hobson, J.A., *REM sleep and dreaming: towards a theory of protoconsciousness.* Nat
962 Rev Neurosci, 2009. **10**(11): p. 803-13.
963 90. Pribbenow, C., et al., *Postsynaptic plasticity of cholinergic synapses underlies the*
964 *induction and expression of appetitive and familiarity memories in Drosophila.* Elife,
965 2022. **11**.
966 91. Barnstedt, O., et al., *Memory-Relevant Mushroom Body Output Synapses Are*
967 *Cholinergic.* Neuron, 2016. **89**(6): p. 1237-1247.
968 92. Melnattur, K., et al., *A conserved role for sleep in supporting Spatial Learning in*
969 *Drosophila.* Sleep, 2020.
970

971 **Figure Legends**

972 **Figure 1. Study rationale and design.** The same genetic background strain (R23E10;UAS-
973 Chrimson) was used for optogenetic or pharmacologically-induced sleep. Flies were fed
974 either all-trans retinal (ATR) or 4,5,6,7-tetrahyrdoisoxazolopyridin-3-ol (THIP) to promote
975 either kind of sleep, which was assessed in three different ways: behavioral analysis, whole
976 brain imaging, and gene expression changes. The comparisons made for each level of
977 analysis are labelled A-E.

978

979 **Figure 2. dFB- and THIP-induced sleep have similar effects on sleep duration and**
980 **consolidation. A)** Experimental regime for observing the effects of dFB activation and THIP
981 provision **(B)**. **C)** Sleep profile across 24 hours in the baseline condition (grey) and dFB
982 activation condition (green). **D)** 3-day average of the 24-hour sleep profile of control (grey)
983 and THIP fed (blue) flies. **E)** Daytime sleep consolidation scatterplot for dFB baseline and
984 THIP control flies. **F)** Daytime sleep consolidation scatterplot for dFB- and THIP-induced
985 sleep. **G)** Night-time sleep consolidation scatterplot for dFB baseline and THIP control flies.
986 **H)** Night-time sleep consolidation scatterplot for dFB- and THIP-induced sleep. n = 87 for
987 dFB activation across three replicates; n = 88 for –THIP, n = 85 for +THIP, across three
988 replicates. See Supplementary Figure 1 for summary histograms and Supplementary Table 1
989 for statistics.

990

991 **Figure 3. Brain imaging during dFB and THIP-induced sleep**

992 **A)** Flies were mounted onto a custom-built holder that allowed a coronal visualization of the
993 brain through the posterior side of the head. Perfusion of extracellular fluid (ECF) occurred
994 throughout all experiments. A 617nm LED was delivered to the brain through the imaging
995 objective during optogenetic experiments. During THIP experiments, 4% THIP in ECF was

perfused onto the brain through a custom perfusion system. Behavior was recorded as the movement of flies on an air suspended ball. **B)** Left: Imaging was carried out across 18 z-slices, with a z-step of 6µm. Each z-plane spanned 667µm x 667µm, which was captured across 256 x 256 pixels. Right: A collapsed mask from one fly of neurons found to be active (green) in C alongside all identified regions of interest (ROIs, gray). **C)** Neural activity in the fly brain, represented across cells (top) and as the population mean (middle) did not change following dFB-induced sleep (bottom). **D)** Neural activity in the fly brain, represented across cells (top) and as the population mean (middle) showed an initial high level of activity in the baseline condition, which decreased when the fly fell asleep (bottom) following THIP exposure.

Figure 4. Brain activity and connectivity decreases during THIP-induced sleep. A) During THIP experiments, ECF +/- THIP was perfused onto the brain of flies. An air puff stimulus was delivered to the fly to test for behavioral responsiveness. **B)** Experimental protocol for behavioral responsiveness experiments (upper). Experimental protocol for imaging experiments is indicated below. 5 mins of baseline condition were recorded, followed by 5 mins of THIP perfusion. Following sleep induction, an additional 10 minutes of calcium activity was recorded, which was separated into 'Early' and 'Mid' sleep for analysis. **C)** Mean behavioral response rate (% ± sem) to air puff stimuli over the course of an experiment (n = 4). Air puff delivery times are indicated by the solid dots. **D)** Percent neurons active (± sem) in non ATR-fed UAS:Chrimson / X ; Nsyb:LexA/+ ; LexOp:nlsGCaMP6f / R23E10:Gal4 flies during wake, THIP-induced sleep, and recovery (n = 9; 3 flies were recorded post-waking). **E)** Correlation analysis (mean degree ± sem) of active neurons in (D). **F)** Collapsed mask of neurons active during wake, and both early and mid THIP sleep. **G)** Overlap in neural identities between wake and THIP-induced sleep in two example flies. Number indicates active neurons within each condition. **H)** Quantification

of neural overlap data. Red dots indicate the flies shown in (F). n = 9 flies. All tests are one-way ANOVA with Dunnett's multiple comparison test. ns = not significant, * = $p<0.05$, ** = $p<0.01$, **** = $p < 0.001$.

Figure 5. Metabolic processes are downregulated during THIP-induced sleep.

A) Schematic representation of the experimental set-up and samples processed using RNA-Sequencing. **B)** Venn diagram showing the gene expression overlap between flies that had been treated with THIP versus their control (shaded blue) and flies that had been treated with THIP in a sleep deprived background versus their control (shaded blue bars). The number of significant differentially-expressed genes in each category is indicated. **C)** Volcano plot representing the distribution of differentially expressed genes in the presence or absence of THIP. Genes that are significantly up/down regulated meeting a Log2Fold change of 0.58 and FDRq value of 0.05 are shown in red. Genes meeting the threshold for FDRq value only are shown in blue. Fold change only is shown in green. Those genes not meeting any predetermined criteria are shown in grey. **D)** Volcano plot representing the distribution of differentially expressed genes in the presence or absence of Gaboxadol in a sleep deprived background. Criteria as above (Figure 5C). **E)** Schematic representation of Gene Ontology (GO) enrichment of biological process results. Colour coded to indicate parent and child terms for comparisons between groups highlighted above (Figure 5C - Left and Figure 5D - Right). **F)** Bar chart representation of a subset of interesting significant GO pathway terms originating from the organic substance and primary metabolic processes for the dataset shown in Figure 5C. **G)** Comparison between significant gene hits obtained via RNA-Sequencing (Blue) and qRT-PCR (Grey) in response to Gaboxadol, represented by Log2Fold change values. See Supplemental Tables 2&3 and Supplementary Figures 2&3.

Figure 6. A variety of biological processes including axon guidance are upregulated during dFB-induced sleep.

A) Schematic representation of the experimental set-up and samples processed using RNA-Sequencing. **B)** Venn diagram showing the gene expression overlap between flies that experienced 10 hours of dFB-induced sleep (ZT10) compared to -ATR controls (ZT10) and those flies where dFB activation was restricted to 1 hour (ZT1) and compared to -ATR controls (ZT1). **C)** Volcano plot representing the distribution of differentially expressed genes resulting from optogenetic dFB activation for 10 hours versus control flies which were allowed to sleep spontaneously for 10 hours. Genes that are significantly up/down regulated meeting a Log2Fold change of 0.58 and FDRq value of 0.05 are shown in red. Genes meeting the threshold for FDRq value only are shown in blue. Fold change only in green. Those genes not meeting any predetermined criteria are shown in grey. **D)** Volcano plot representing the distribution of differentially expressed genes resulting from optogenetic dFB activation for 1 hour versus control flies which were allowed to sleep spontaneously for 1 hour. Criteria as above (Figure 6C). **E)** Schematic representation of Gene Ontology (GO) enrichment of biological process results. Color coded to indicate parent and child terms comparing flies that had been activated optogenetically for 10 hours versus flies which had been allowed to spontaneously sleep for the same duration. **F)** Bar chart representation of a subset of interesting significant GO pathway terms originating from the regulation of cellular processes and signalling biological processes. **G)** Comparison between significant gene hits obtained via RNA-Sequencing (Green) and qRT-PCR (Grey) in response to optogenetic sleep, represented by Log2Fold change values. See Supplemental Tables 4-7 and Supplementary Figures 4&5.

Figure 7. nAchRα subunit knockouts bidirectionally regulate >5min sleep as well as short sleep. A. Average total day and night sleep duration (minutes±95% confidence intervals) in nAchRα knockout mutants, expressed as difference to their respective background controls (see Methods). α1, N=91; contro1 ($X^{59}w^{1118}$) = 93; α2, N=70; control (w^{1118}ActinCas9) = 65; α3, N=43; (ActinCas9) =9; α4, N=87; (w^{1118}ActinCas9) =98; α6, N=91; (w^{1118}ActinCas9) =91; α7, N=94; (ActinCas9) =95. *P<0.01, ***P<0.001, ****P<0.0001 by t-test adjusted for multiple comparisons. **B.** Left two panels: sleep architecture for the same six knockout strains as in A (green), shown against their respective controls (black). Each datapoint is a fly. Right panels: cumulative short sleep (1-5min) expressed as a percentage of total sleep duration. Data are the from the same experiment as in Figure A&B. Each datapoint is a fly. **P<0.01, ***P<0.001, ****P<0.0001 Man-Whitney U Test. All data were collected over three days and three nights and averaged.

Figure 8. AkhR knockdown decreases >5min sleep but not short sleep. A,B. Total sleep (>5min) in UAS-AkhR:RNAi / R57C10-Gal4 flies (blue, N=126) compared to genetic controls (light grey: UAS-AkhR:RNAi / + , N= 124; dark grey: R57C10-Gal4 / + , N= 120). **C.** Sleep architecture (average bout duration versus bout number per fly) in data from A,B. **D.** Cumulative short sleep (1-5min, expressed as a % of total sleep) in UAS-AkhR:RNAi / R57C10-Gal4 flies (blue) compared to genetic controls (light grey: UAS-AkhR:RNAi / + ; dark grey: R57C10-Gal4 / +). Wild-type background (+) is Canton-S(w^{1118}). Each datapoint is a fly. ***P<0.001, ****P<0.0001 Man-Whitney U Test. ns, not significant. All data were collected over two days and two nights and averaged.

Supplementary Figure Legends

Figure S1. Sleep architecture in dFB and THIP induced sleep (related to Figure 2).

A-B. Average number of sleep bouts in control (grey) and dFB activation (green) conditions in the day and night for both +ATR **(A)** and –ATR **(B)** fed flies. dFB-induced sleep results in an increase in the number of sleep bouts both during the day and the night, whereas red light alone has no effect. **C-D.** dFB activation (green) increases the average sleep duration during the day, but not the night when compared to controls (grey) in +ATR flies **(C)**. **D.** –ATR flies show no difference in mean sleep bout duration during the day, but show a decrease in average bout duration during the night. THIP (blue) increases both the average number of sleep bouts **(E)** and the average duration of sleep bouts **(F)** during the day, but not the night, when compared to controls (grey). Analysis for a and b = Kruskal-Wallis test with Dunn's multiple comparison correction. * = $p<0.05$, *** = $p < 0.001$, **** = $p<0.0001$. For e and f, analysis = Ordinary one-way ANOVA with Tukey correction for multiple comparisons. *** = $p<0.001$, **** = $p <0.0001$.

Figure S2. Gene Ontology (GO) enrichment analysis for THIP-induced sleep (related to Figure 5). Significantly downregulated and upregulated GO categories for THIP-sleep (Table S2), listed from most enriched at the top. Broad GO categories are identified below.

Figure S3. Gene Ontology (GO) enrichment analysis for THIP-provisioned flies that were sleep deprived (related to Figure 5). Significantly downregulated and upregulated GO categories for sleep deprived flies (Table S3), listed from most enriched at the top. Broad GO categories are identified below.

Figure S4. Gene Ontology (GO) enrichment analysis for dFB-induced sleep (related to Figure 7). Significantly downregulated and upregulated GO categories for dFB-sleep (Table S4), listed from most enriched at the top. Broad GO categories are identified below.

Figure S5. Circadian-related genes uncovered in dFB-sleep dataset (related to Figure 7). **A.** Zeitgeber (ZT) 10 timepoint was compared with ZT in to uncover potential circadian-regulated genes, in two separate datasets (-ATR and +ATR). 98 genes were shared between these datasets. **B.** Of the 98 shared genes, circadian-related processes were highly enriched. **C.** Expression levels of 7 circadian genes drawn from the two different datasets in A.

Figure S6. Summary of different Gene Ontogeny pathways engaged by dFB-induced sleep and THIP-induced sleep. A. Either sleep induction method produces different levels of activity in the fly brain. WE term dFB-induced sleep ‘active sleep’ because brain activity levels are not different than during wake. We term THIP-induced sleep ‘quiet sleep’ because neural activity is significant decreased already in the first 5 minutes. Both of these induced forms of sleep resemble sleep stages seen during spontaneous sleep in flies. **B.** Number of GO pathways engaged by either induced active or quiet sleep, separated by upregulated versus downregulated biological processes.

Supplementary Tables

Table S1, related to Figure 2. A comparison of sleep duration profiles (min/hr) during dFB and THIP induced sleep. Tested with 2way ANOVA with Tukey's multiple comparison test.

Table S2, related to Figure 5. List of significant THIP-sleep genes.

Table S3, related to Figure 5. List of significant sleep-deprivation genes in THIP-fed flies.

Table S4, related to Figure 6. List of significant dFB-sleep genes after 10 hours activation.

Table S5, related to Figure 6. List of significant dFB-sleep genes after 1 hour of activation.

Table S6, related to Figure 6. List of significant ZT10 vs ZT1 genes in ATR+ dataset.

Table S7, related to Figure 6. List of significant ZT10 vs ZT1 genes in ATR- dataset.

Table S8, related to Figures 5 & 6. Primer list for RT qPCR validation experiments.

Background R23e10Gal4 > UAS-Chrimson

Sleep Manipulation Optogenetic Pharmacological

Treatment	-ATR	+ATR	+THIP	-THIP
	Control	Sleep	Sleep	Control

Sleep Readout Comparisons

1. Behaviour

2. Brain Activity

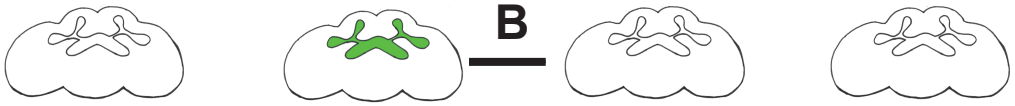

3. Transcriptome

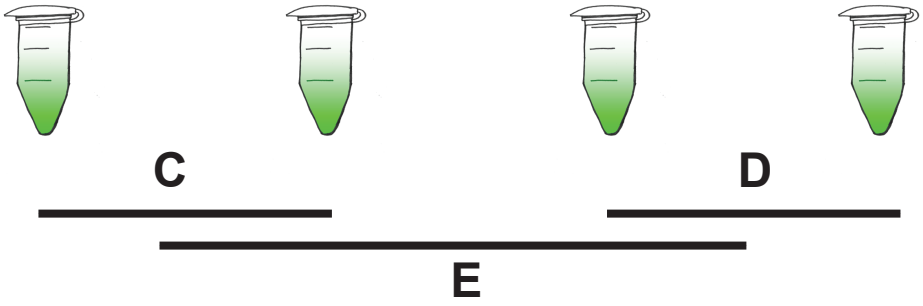

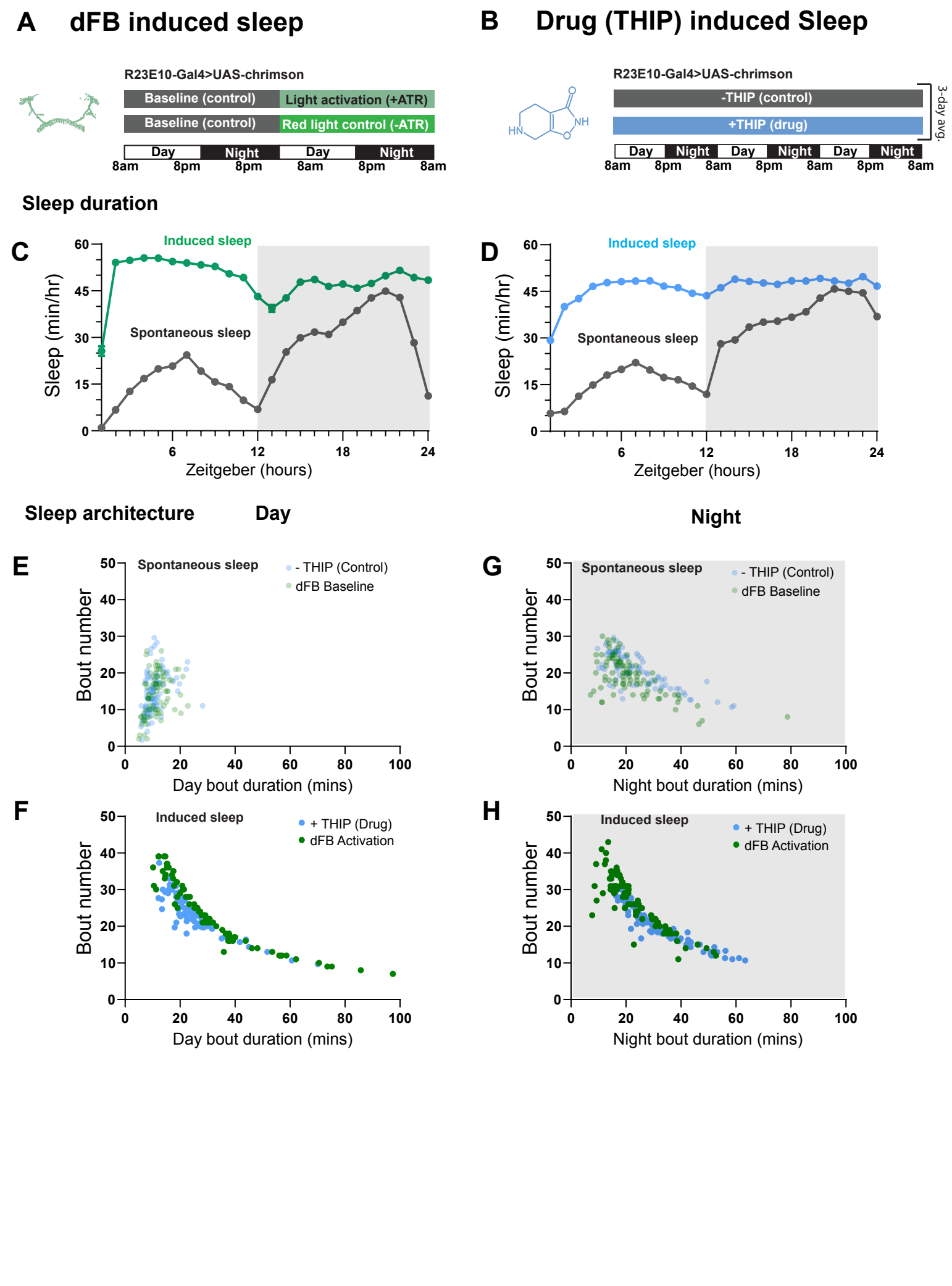

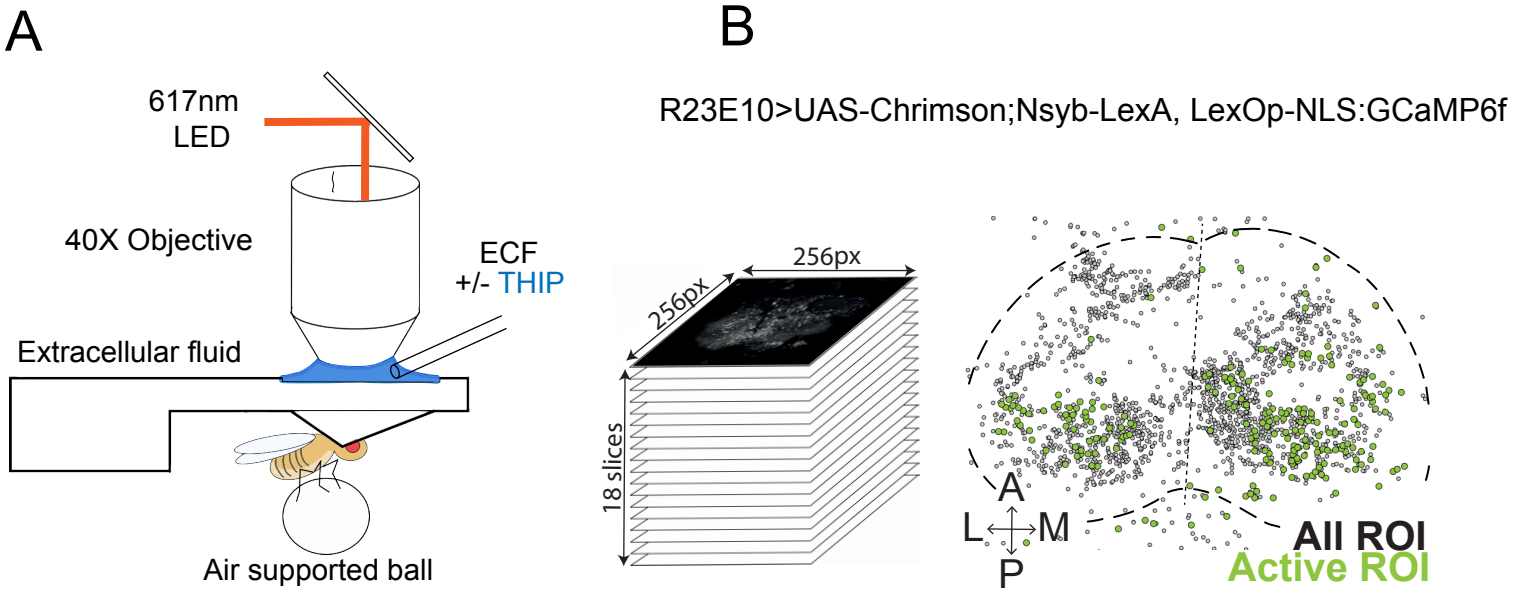

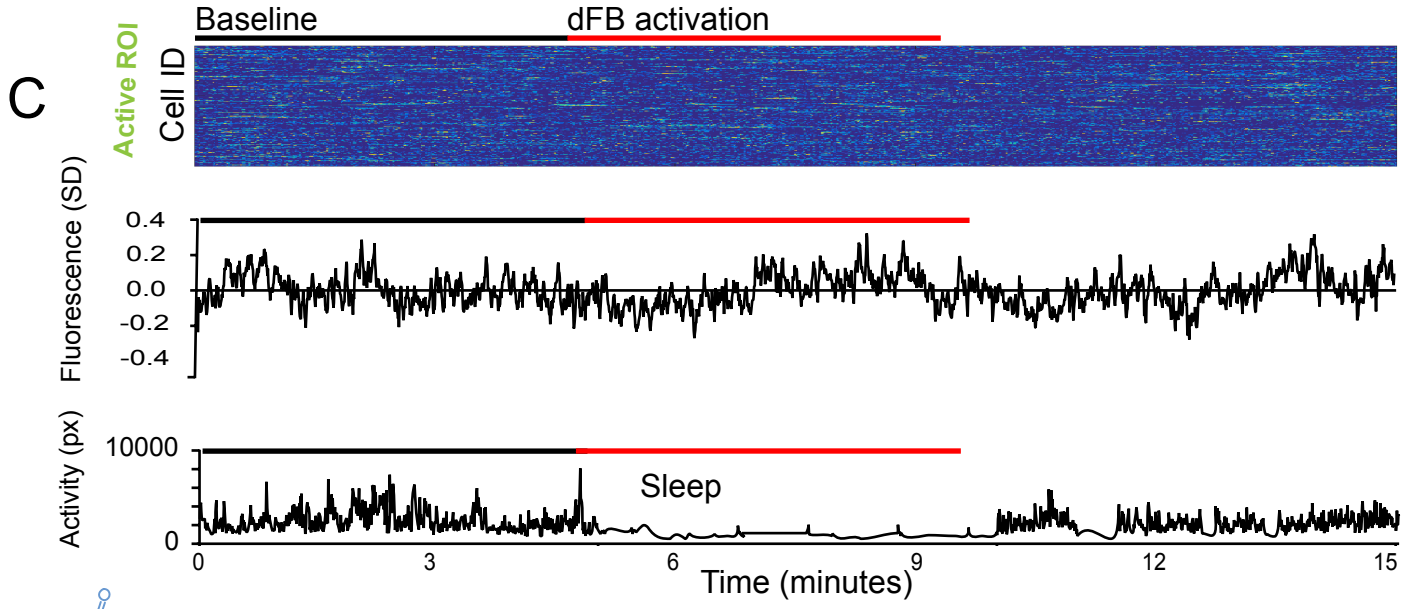

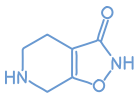

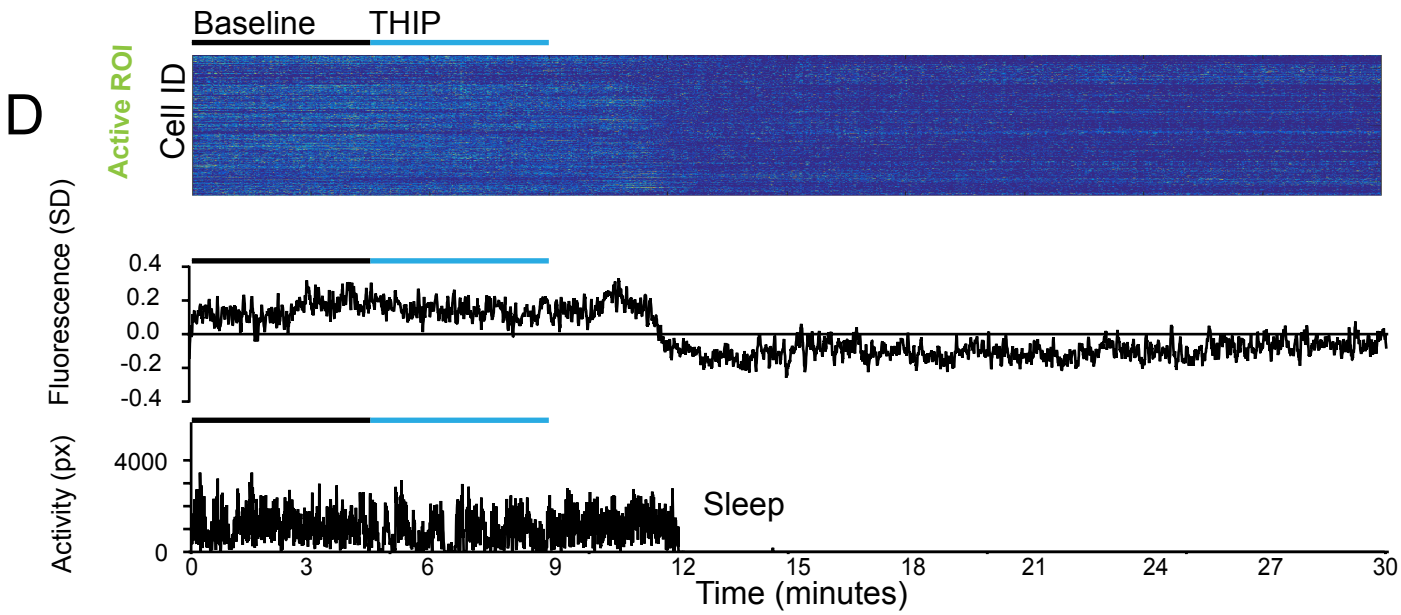

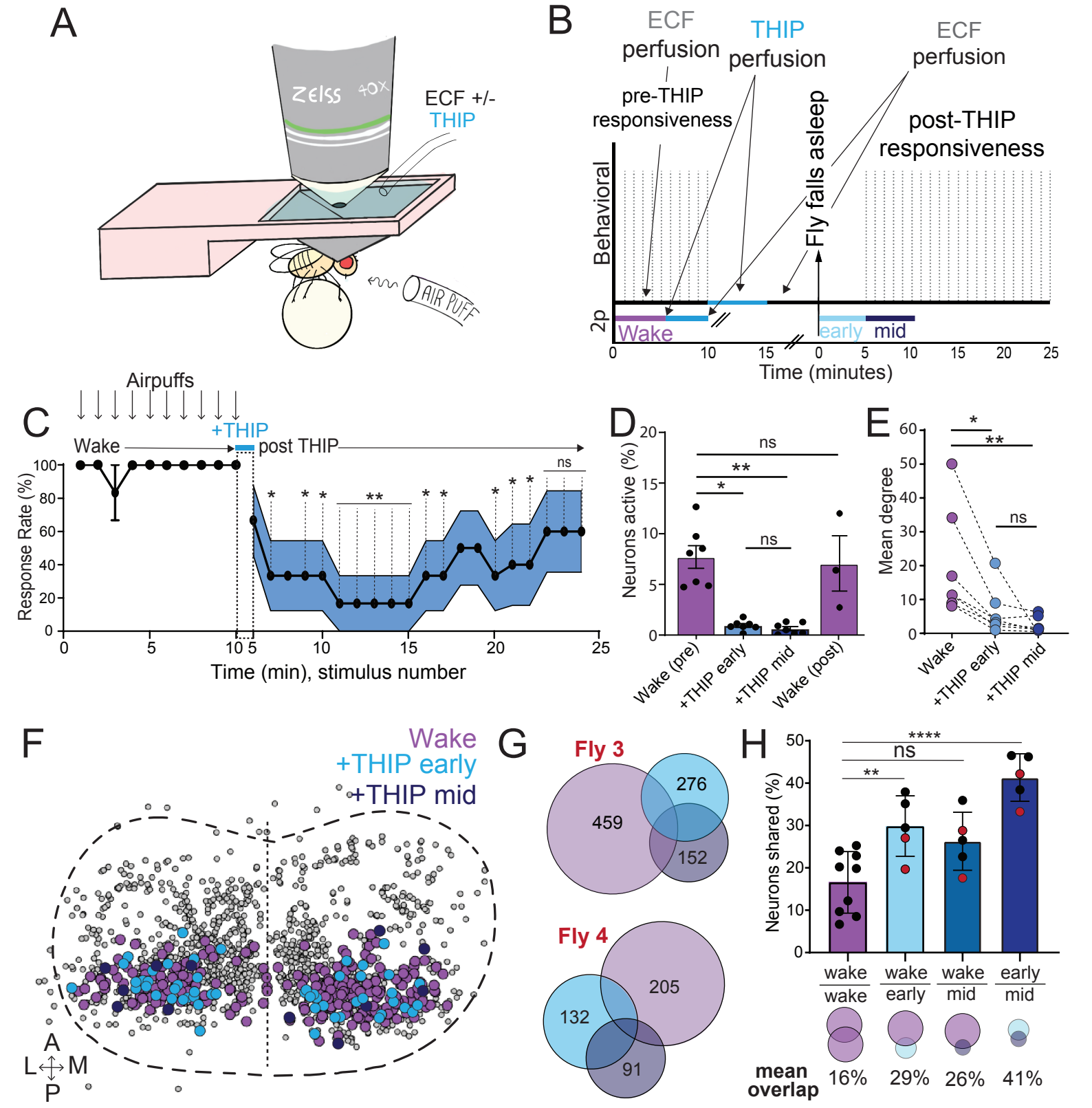

Figure 5

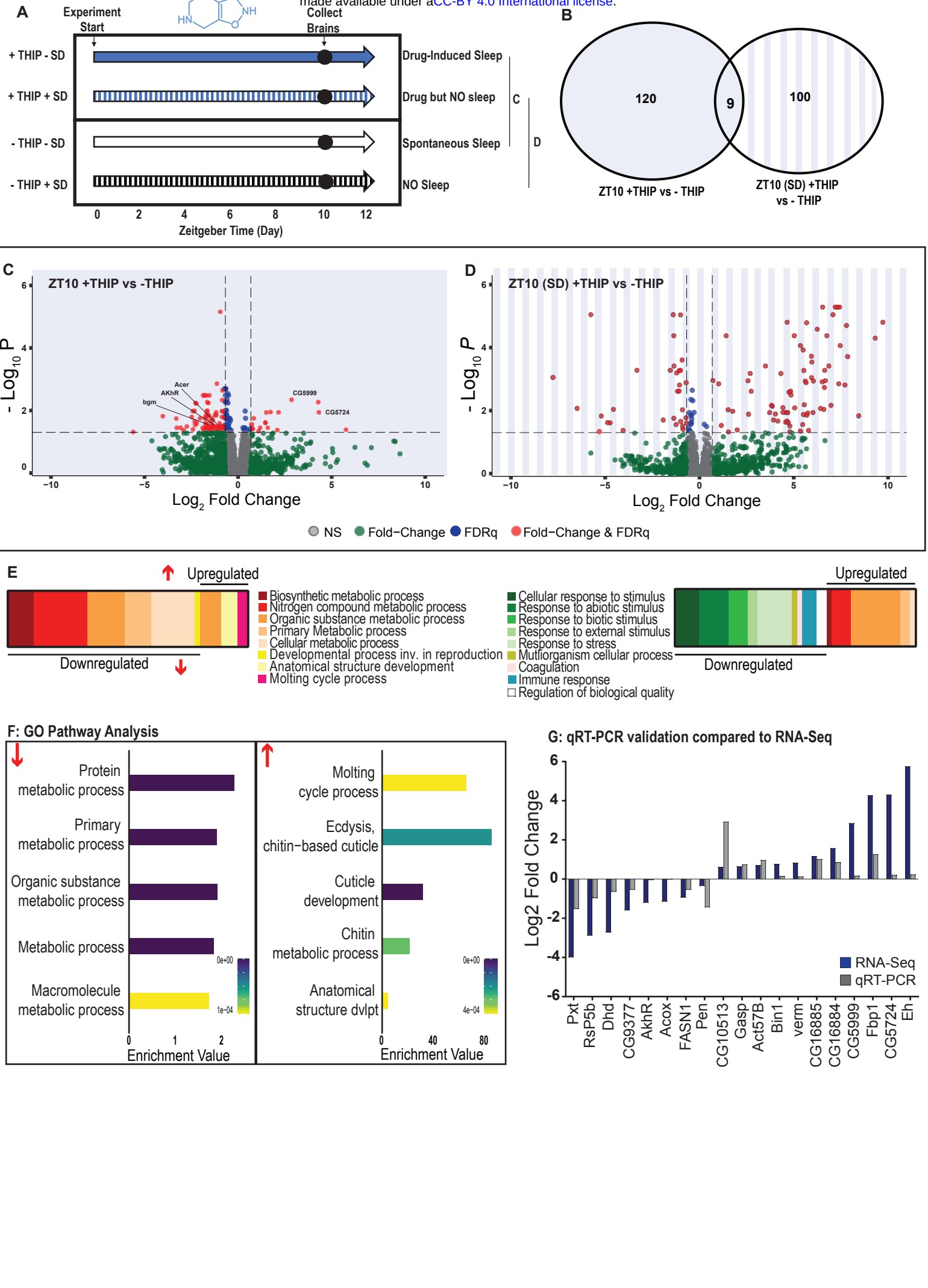

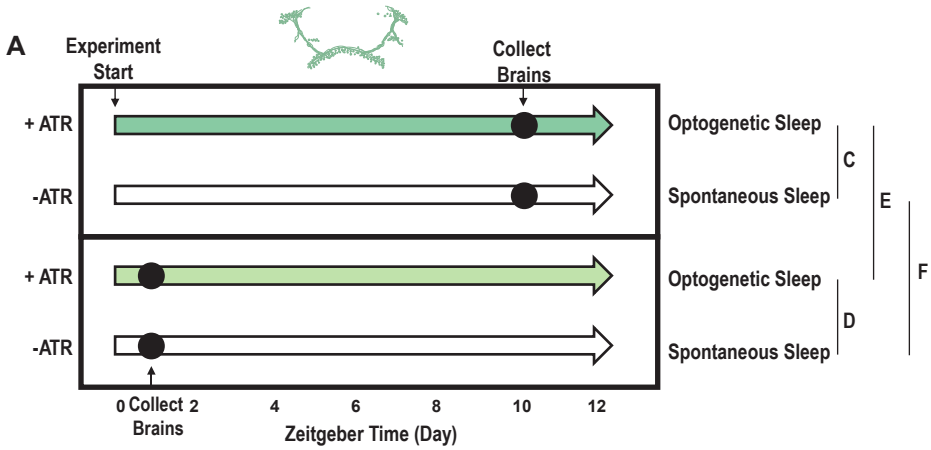

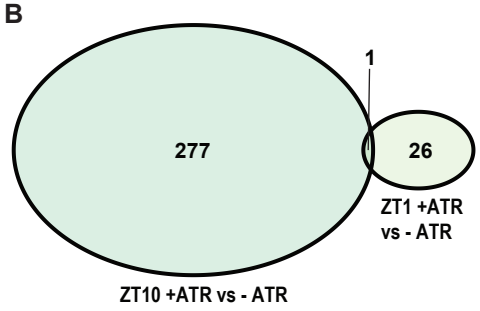

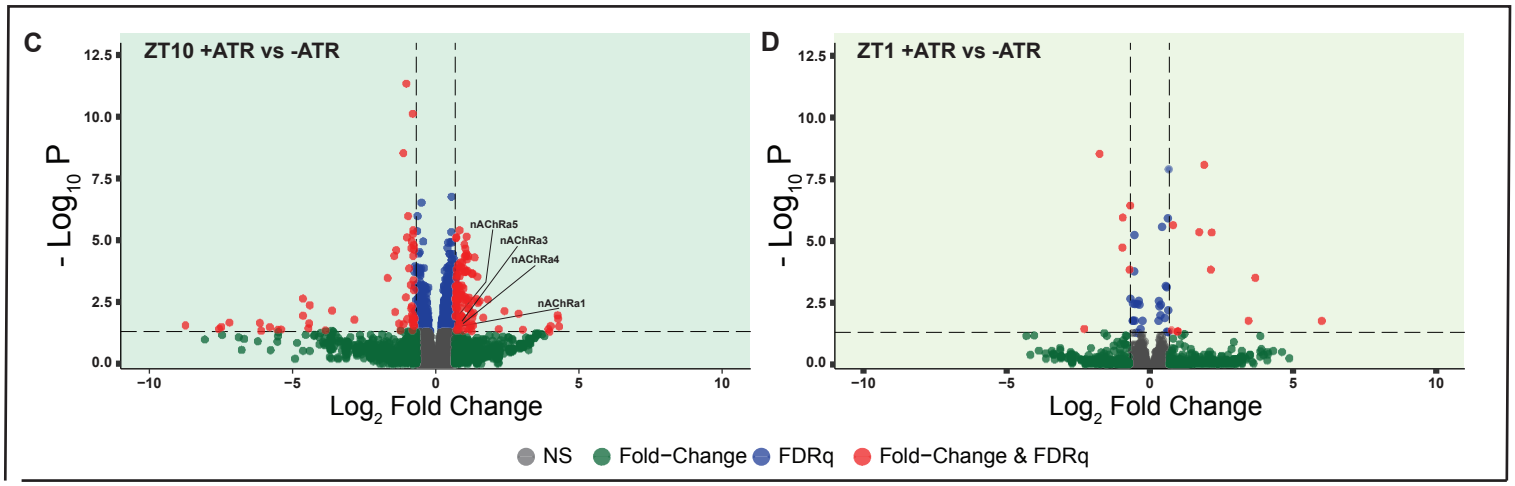

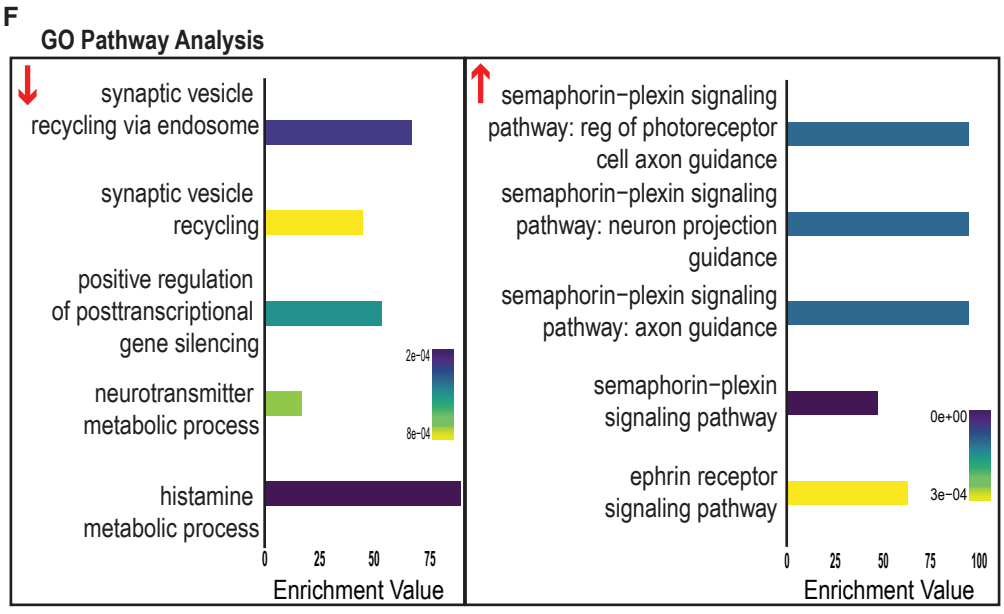

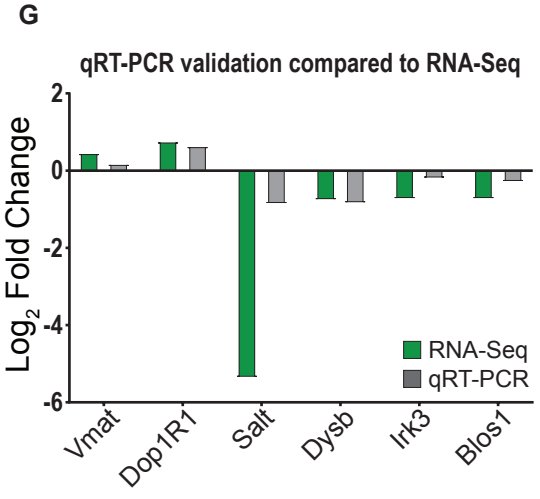

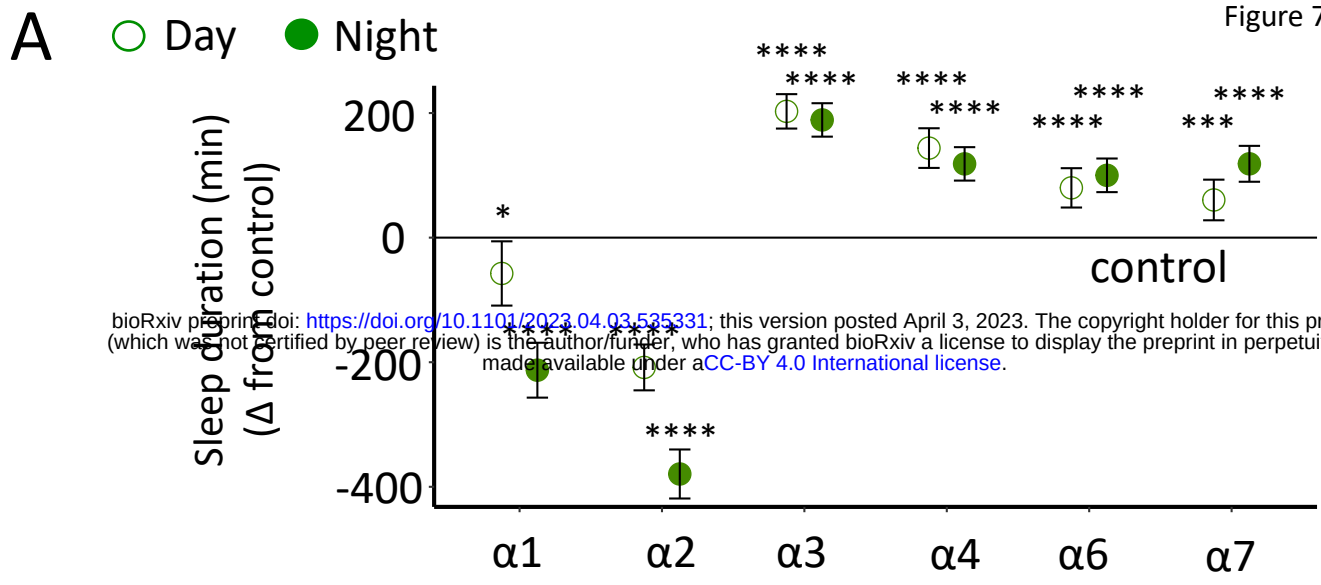

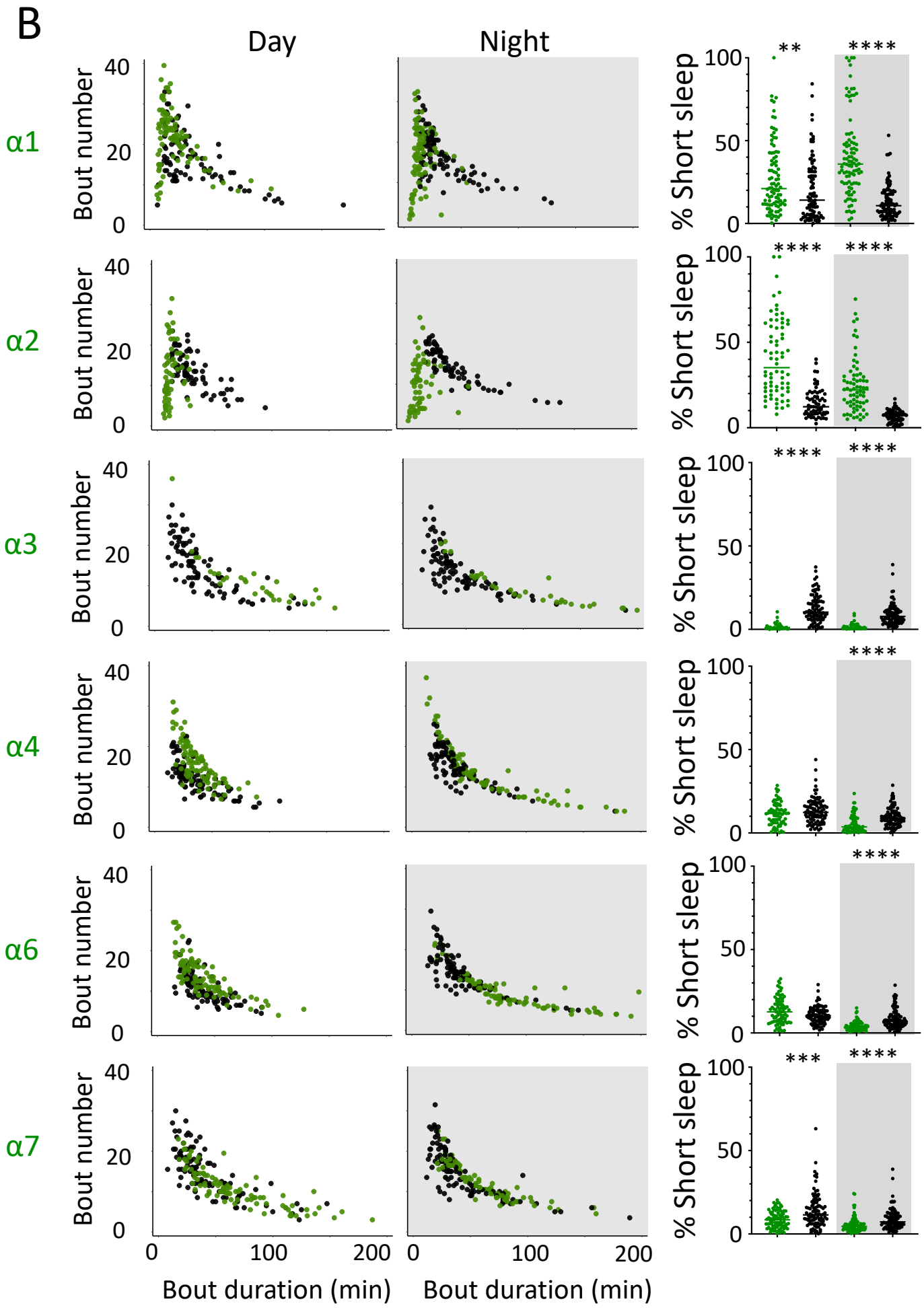

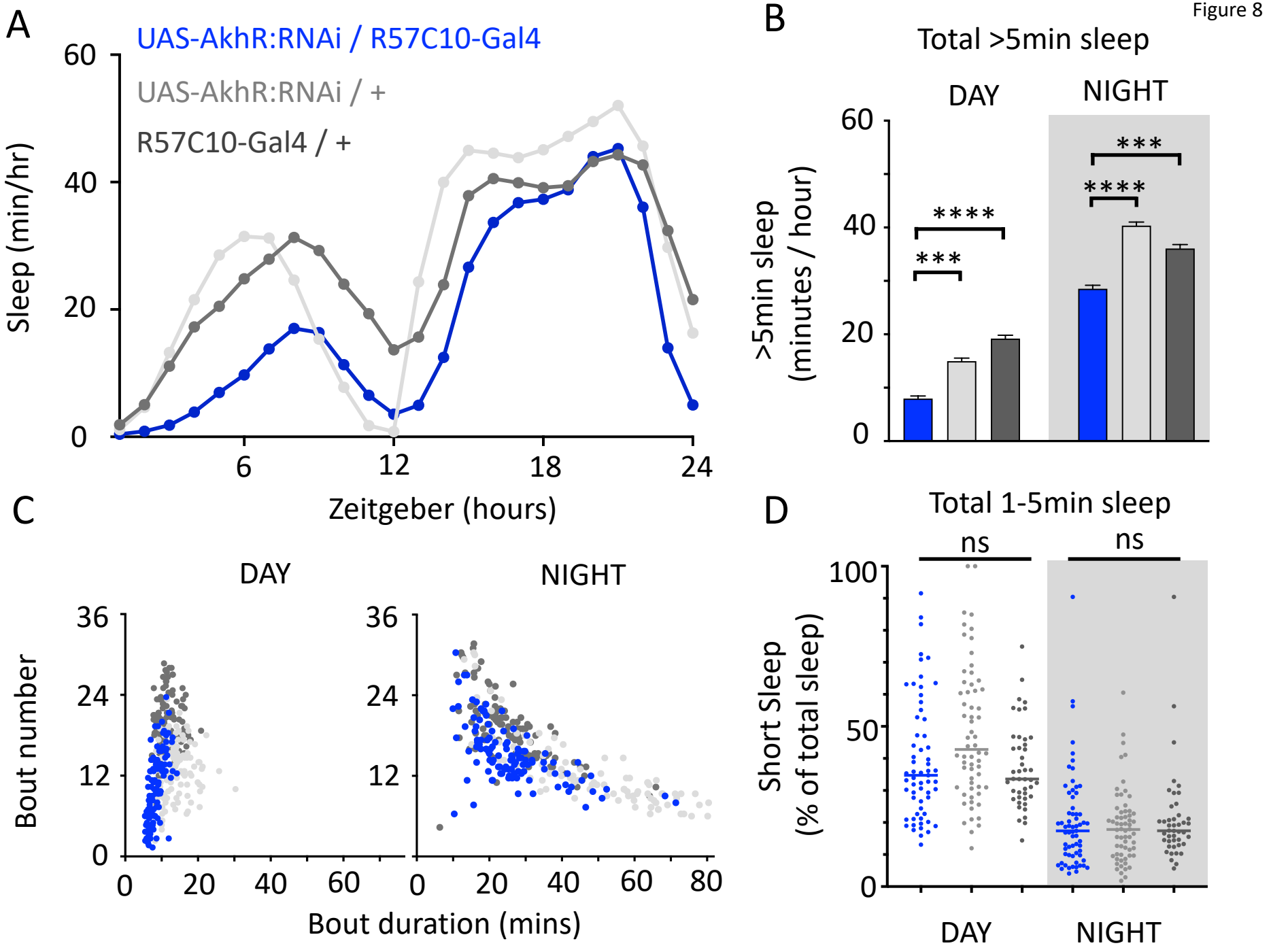
A
UAS-AkhR:RNAi / R57C10-Gal4
UAS-AkhR:RNAi / +
R57C10-Gal4 / +
Sleep (min/hr)
60
40
20
0
6
12
18
24
Zeitgeber (hours)
B
Total >5min sleep
DAY
NIGHT
>5min sleep (minutes / hour)
60
40
20
0
****
***
****
***
C
DAY
NIGHT
Bout number
36
24
12
0
0
20
40
60
80
Bout duration (mins)
D
Total 1-5min sleep
ns
ns
Short Sleep (% of total sleep)
100
50
0
DAY
NIGHT

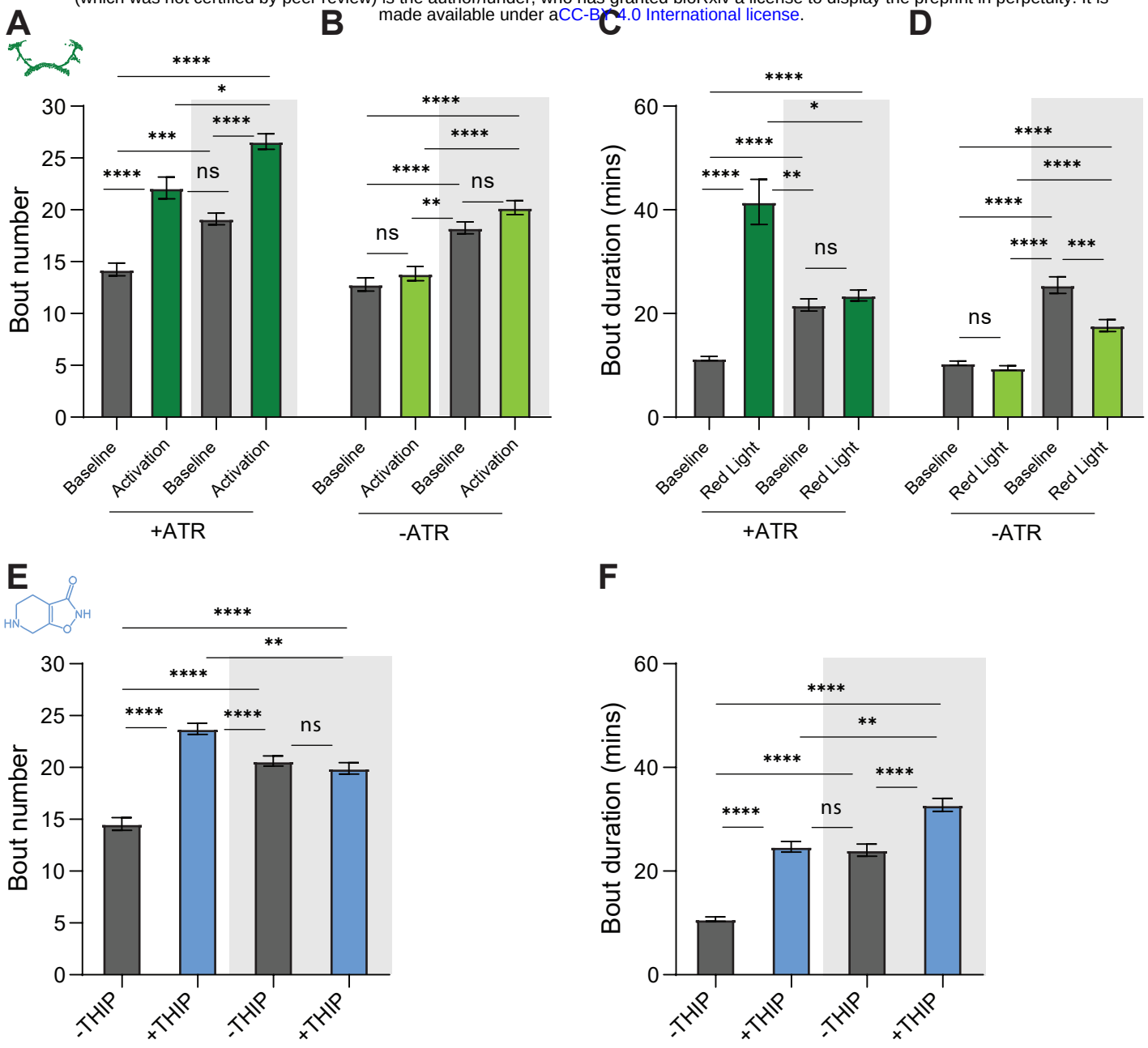

	GO Term	Pvalue	Enrichment value
Downregulated	GO:0046460 neutral lipid biosynthetic process	0.0006	52.92
	GO:0046463 acylglycerol biosynthetic process	0.0006	52.92
	GO:0002181 cytoplasmic translation	0.0000	33.41
	GO:0009059 macromolecule biosynthetic process	0.0000	6.44
	GO:0009058 biosynthetic process	0.0000	4.53
	GO:0009064 glutamine family amino acid metabolic process	0.0008	16.54
	GO:0006412 translation	0.0000	11.7
	GO:0043043 peptide biosynthetic process	0.0000	11.54
	GO:0043604 amide biosynthetic process	0.0000	10.48
	GO:0006518 peptide metabolic process	0.0000	8.89
	GO:1901566 organonitrogen compound biosynthetic process	0.0000	6.38
	GO:0044271 cellular nitrogen compound biosynthetic process	0.0000	5.07
	GO:0034641 cellular nitrogen compound metabolic process	0.0000	2.31
	GO:1901564 organonitrogen compound metabolic process	0.0000	2.06
	GO:0006807 nitrogen compound metabolic process	0.0002	1.6
	GO:1901576 organic substance biosynthetic process	0.0000	4.53
	GO:0019752 carboxylic acid metabolic process	0.0008	3.36
	GO:0043436 oxoacid metabolic process	0.0010	3.26
	GO:0006082 organic acid metabolic process	0.0010	3.25
	GO:0019538 protein metabolic process	0.0000	2.27
	GO:0071704 organic substance metabolic process	0.0000	1.9
	GO:0043170 macromolecule metabolic process	0.0001	1.72
	GO:0006591 ornithine metabolic process	0.0006	52.92
	GO:0006525 arginine metabolic process	0.0008	44.1
	GO:1901605 alpha-amino acid metabolic process	0.0003	6.73
	GO:0008152 metabolic process	0.0000	1.83
	GO:0044238 primary metabolic process	0.0000	1.89
	GO:0019432 triglyceride biosynthetic process	0.0003	66.15
	GO:0006414 translational elongation	0.0000	34.51
	GO:0034645 cellular macromolecule biosynthetic process	0.0000	7.55
	GO:0043603 cellular amide metabolic process	0.0000	7.7
	GO:0044249 cellular biosynthetic process	0.0000	4.69
	GO:0044267 cellular protein metabolic process	0.0000	2.58
	GO:0044260 cellular macromolecule metabolic process	0.0000	2.02
	GO:0044237 cellular metabolic process	0.0000	1.67
	GO:0007548 sex differentiation	0.0003	22.05
Upregulated	GO:0006030 chitin metabolic process	0.0003	21.44
	GO:1901071 glucosamine-containing compound metabolic process	0.0004	19.78
	GO:0006040 amino sugar metabolic process	0.0004	19.33
	GO:0006022 aminoglycan metabolic process	0.0006	17.48
	GO:0018990 ecdysis, chitin-based cuticle	0.0002	85.05
	GO:0022404 molting cycle process	0.0004	65.42
	GO:0040003 chitin-based cuticle development	0.0000	32.89
	GO:0042335 cuticle development	0.0000	31.33
	GO:0048856 anatomical structure development	0.0004	4.39

Metabolic process

- **Biosynthetic metabolic process**
- **Nitrogen compound metabolic process**
- **organic substance metabolic process**
- **primary metabolic process**
- **Cellular metabolic process**

Developmental Process

- **Developmental process involved in reproduction**
- **Anatomical structure development**

Mutlicellular organismal process

- **Molting cycle process**

	GO Term	Pvalue	Enrichment value
Downregulated	GO:0104004 cellular response to environmental stimulus	0.0005	19.04
	GO:0050896 response to stimulus	0.0000	3.79
	GO:0034644 cellular response to UV	0.0000	85.05
	GO:0009411 response to UV	0.0001	41.15
	GO:0071482 cellular response to light stimulus	0.0001	32.71
	GO:0071478 cellular response to radiation	0.0003	22.78
	GO:0071214 cellular response to abiotic stimulus	0.0005	19.04
	GO:0009266 response to temperature stimulus	0.0000	16.88
	GO: 0009617 response to bacterium	0.0000	21.07
	GO: 0051707 response to other organism	0.0000	15.39
	GO:0043207 response to external biotic stimulus	0.0000	15.14
	GO: 0009607 response to biotic stimulus	0.0000	15.09
	GO:0050830 defense response to Gram-positive bacterium	0.0000	36.98
	GO:0009605 response to external stimulus	0.0000	9.31
	GO:0034605 cellular response to heat	0.0000	60.75
	GO:0009408 response to heat	0.0000	26.58
	GO:0006979 response to oxidative stress	0.0002	13.83
	GO:0042742 defense response to bacterium	0.0000	12.89
	GO:0098542 defense response to other organism	0.0000	11.63
	GO:0006952 defense response	0.0000	10.12
	GO:0006950 response to stress	0.0000	5.79
	GO:0042381 hemolymph coagulation	0.0001	141.75
	GO:0006955 immune response	0.0007	9.83
	GO:0002376 immune system process	0.0002	9.01
	GO:0007599 hemostasis	0.0001	141.75
	GO:0050878 regulation of body fluid levels	0.0005	56.7
	GO:0051704 multi-organism process	0.0000	12.34
	GO:0050817 coagulation	0.0001	141.75
Upregulated	GO:0008152 metabolic process	0.0000	1.86
	GO:0006032 chitin catabolic process	0.0001	36.6
	GO:1901072 glucosamine-containing compound catabolic process	0.0001	32.53
	GO:0006022 aminoglycan metabolic process	0.0000	13.37
	GO:0006807 nitrogen compound metabolic process	0.0000	1.94
	GO:0046348 amino sugar catabolic process	0.0001	32.53
	GO:0006026 aminoglycan catabolic process	0.0003	21.69
	GO:0006030 chitin metabolic process	0.0000	16.4
	GO:1901071 glucosamine-containing compound metabolic process	0.0000	15.13
	GO:0006040 amino sugar metabolic process	0.0000	14.79
	GO:0006508 proteolysis	0.0000	5.13
	GO:1901135 carbohydrate derivative metabolic process	0.0002	3.94
	GO:1901564 organonitrogen compound metabolic process	0.0000	2.31
	GO:0043170 macromolecule metabolic process	0.0000	2.1
	GO:0071704 organic substance metabolic process	0.0000	1.92
	GO:0019538 protein metabolic process	0.0008	2.01
	GO:0044238 primary metabolic process	0.0004	1.67
	GO:0017144 drug metabolic process	0.0000	6.24

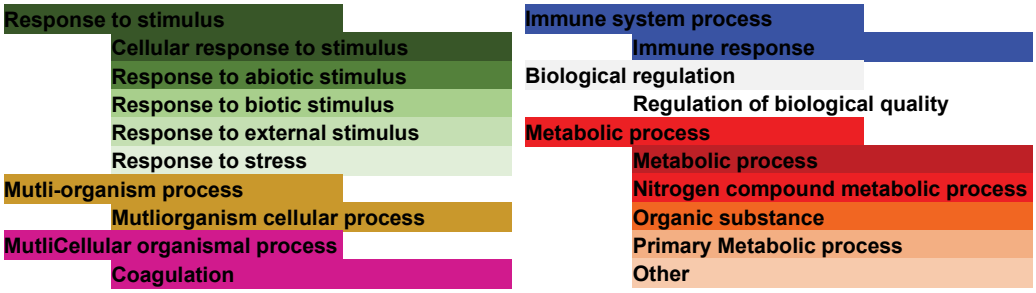

	GO Term	Pvalue	Enrichment value
Downregulated	GO:0060148 positive regulation of posttranscriptional gene silencing	0.0005	53.51
	GO:0002181 cytoplasmic translation	0	9.46
	GO:0052803 imidazole-containing compound metabolic process	0.0002	89.19
	GO:0001692 histamine metabolic process	0.0002	89.19
	GO:0042133 neurotransmitter metabolic process	0.0007	16.72
	GO:1900368 regulation of RNA interference	0.0001	133.79
	GO:1900370 positive regulation of RNA interference	0.0001	133.79
	GO:0036466 synaptic vesicle recycling via endosome	0.0003	66.89
	GO:0036465 synaptic vesicle recycling	0.0008	44.6
Upregulated	GO:2000766 negative regulation of cytoplasmic translation	0.0003	63.5
	GO:0017148 negative regulation of translation	0.0002	9.16
	GO:0034249 negative regulation of cellular amide metabolic process	0.0004	7.81
	GO:0006417 regulation of translation	0.0001	5.69
	GO:0034248 regulation of cellular amide metabolic process	0.0001	4.68
	GO:0010608 posttranscriptional regulation of gene expression	0.0001	4.61
	GO:0010468 regulation of gene expression	0	2.21
	GO:0031326 regulation of cellular biosynthetic process	0.0001	2.04
	GO:0009889 regulation of biosynthetic process	0.0001	2.04
	GO:0010556 regulation of macromolecule biosynthetic process	0.0004	1.98
	GO:0060255 regulation of macromolecule metabolic process	0.0001	1.86
	GO:0019222 regulation of metabolic process	0.0001	1.81
	GO:0051171 regulation of nitrogen compound metabolic process	0.0005	1.76
	GO:0080090 regulation of primary metabolic process	0.0006	1.74
	GO:0031323 regulation of cellular metabolic process	0.0007	1.71
	GO:0046011 regulation of oskar mRNA translation	0	29.31
	GO:1902287 semaphorin-plexin signaling pathway involved in axon guidance	0.0001	95.26
	GO:1902285 semaphorin-plexin signaling pathway involved in neuron projection guidance	0.0001	95.26
	GO:0045876 positive regulation of sister chromatid cohesion	0.0001	95.26
	GO:2000305 semaphorin-plexin signaling pathway involved in reg of photoreceptor cell axon guidance	0.0001	95.26
	GO:0048013 ephrin receptor signaling pathway	0.0003	63.5
	GO:0071526 semaphorin-plexin signaling pathway	0	47.63
	GO:0007162 negative regulation of cell adhesion	0.0006	17.86
	GO:0051128 regulation of cellular component organization	0.0002	2.4
	GO:0048522 positive regulation of cellular process	0.0007	1.88
	GO:0099177 regulation of trans-synaptic signaling	0.0001	5.82
	GO:0050804 modulation of chemical synaptic transmission	0.0001	5.82
	GO:0016319 mushroom body development	0.001	6.52
	GO:2000026 regulation of multicellular organismal development	0.0007	2.57
	GO:0032502 developmental process	0.0001	1.81
	GO:0032879 regulation of localization	0.0006	2.72
	GO:2000112 regulation of cellular macromolecule biosynthetic process	0.0004	1.98
	GO:0050794 regulation of cellular process	0	1.84
	GO:0048518 positive regulation of biological process	0.0008	1.8
	GO:0050789 regulation of biological process	0	1.7
	GO:0065007 biological regulation	0	1.63
	GO:0042391 regulation of membrane potential	0.0008	6.9
	GO:0065008 regulation of biological quality	0.0002	2.12
	GO:0120187 positive regulation of protein localization to chromatin	0.0001	95.26
	GO:0008049 male courtship behavior	0.0003	8.36
	GO:0060179 male mating behavior	0.0005	7.56

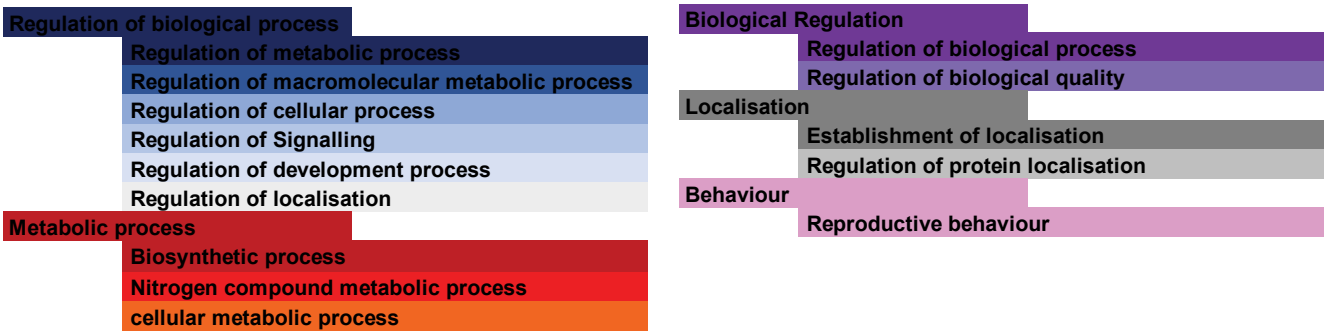

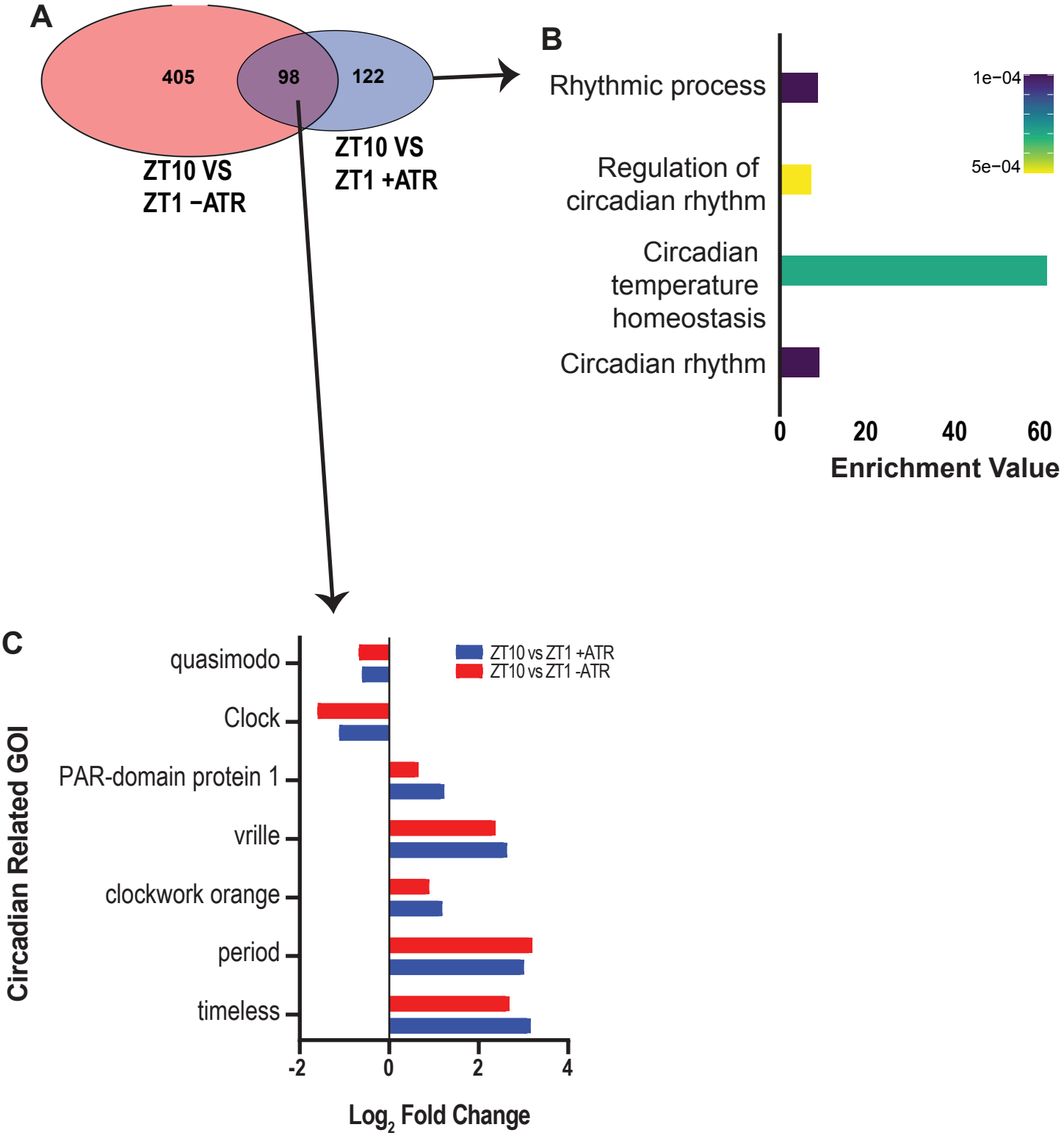

A: Sleep induction method

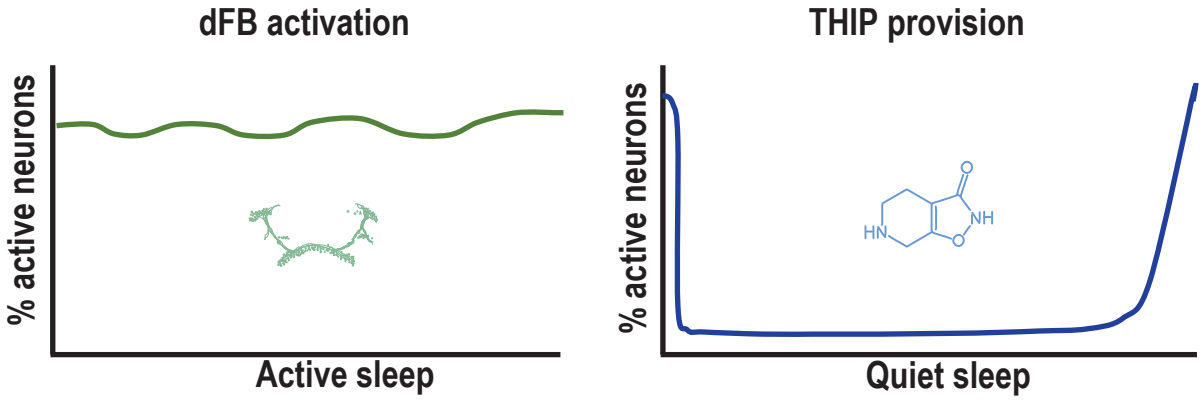

B: Induced Sleep Transcriptome: GO Pathways of Biological Processes